MT1-MMP targeting to endolysosomes is mediated by upregulation of flotillins

Damien Planchon, Eduardo Rios Morris, Mallory Genest, Franck Comunale, Sophie Vacher, Ivan Bièche, Evgeny Denisov, Lubov Tashireva, Vladimir Perelmuter, Stefan Linder, et al.

© 2018. Published by The Company of Biologists Ltd | Journal of Cell Science (2018) 131, jcs218925. doi:10.1242/jcs.218925

RESEARCH ARTICLE

MT1-MMP targeting to endolysosomes is mediated by upregulation of flotillins

Damien Planchon[1], Eduardo Rios Morris[1], Mallory Genest[1], Franck Comunale[1], Sophie Vacher[2], Ivan Bièche[2], Evgeny V. Denisov[3,4], Lubov A. Tashireva[3], Vladimir M. Perelmuter[3], Stefan Linder[5], Philippe Chavrier[6], Stéphane Bodin[1,*] and Cécile Gauthier-Rouvière[1,*,‡]

ABSTRACT

Tumor cell invasion and metastasis formation are the major cause of death in cancer patients. These processes rely on extracellular matrix (ECM) degradation mediated by organelles termed invadopodia, to which the transmembrane matrix metalloproteinase MT1-MMP (also known as MMP14) is delivered from its reservoir, the RAB7-containing endolysosomes. How MT1-MMP is targeted to endolysosomes remains to be elucidated. Flotillin-1 and -2 are upregulated in many invasive cancers. Here, we show that flotillin upregulation triggers a general mechanism, common to carcinoma and sarcoma, which promotes RAB5-dependent MT1-MMP endocytosis and its delivery to RAB7-positive endolysosomal reservoirs. Conversely, flotillin knockdown in invasive cancer cells greatly reduces MT1-MMP accumulation in endolysosomes, its subsequent exocytosis at invadopodia, ECM degradation and cell invasion. Our results demonstrate that flotillin upregulation is necessary and sufficient to promote epithelial and mesenchymal cancer cell invasion and ECM degradation by controlling MT1-MMP endocytosis and delivery to the endolysosomal recycling compartment.

KEY WORDS: Cancer cell invasion, Extracellular matrix degradation, Endolysosomal vesicular trafficking, Flotillin, MT1-MMP

INTRODUCTION

Metastasis formation, the major cause of death in patients with cancer, is a complex process that starts with the dissemination of cancer cells from the primary tumor. During this process, cancer cells interact with and remodel the extracellular matrix (ECM), notably through its degradation. Amongst all matrix metalloproteases (MMPs), the transmembrane MT1-MMP (also known as MMP14) plays a pivotal role in tumor cell invasion. Once exposed on the cell surface, MT1-MMP can cleave multiple matrix components and also proteolytically activate other MMPs, thus constituting a master regulator of ECM degradation. Many studies demonstrate that tumor cells hijack MT1-MMP trafficking to increase its activity at degradation sites called invadopodia (reviewed in Castro-Castro et al., 2016; Frittoli et al., 2011; Poincloux et al., 2009). Data obtained using different carcinoma and sarcoma cell lines indicate that MT1-MMP endocytic/exocytic fluxes are crucial for its activity. Indeed, activated MT1-MMP has to be internalized and stored in intracellular compartments to be efficiently recycled to invadopodia. Particularly, in invasive cancer cells, a RAB7-positive endolysosomal compartment was identified as the MT1-MMP reservoir compartment, from which polarized trafficking of internalized MT1-MMP to invadopodia occurs (Chevalier et al., 2016; Hoshino et al., 2013; Macpherson et al., 2014; Monteiro et al., 2013; Steffen et al., 2008; Williams and Coppolino, 2011; Yu et al., 2012). The mechanisms of MT1-MMP-polarized exocytosis from the endolysosomal compartment to invadopodia have been recently identified. However, how MT1-MMP is localized from the plasma membrane (PM) to the endolysosomal reservoir compartment in tumor cells remains to be elucidated.

Flotillin-1 and flotillin-2 (hereafter referred to as 'flotillins') are two ubiquitous, highly conserved homologous proteins (Rivera-Milla et al., 2006). They preferentially assemble to form heterotetramers composed of two flotillin-1 and two flotillin-2 molecules localized at the membrane cytoplasmic face and associated with caveolin-independent membrane microdomains enriched in cholesterol and sphingolipids. Flotillin heterotetramers can assemble into large oligomers to form molecular scaffolds (Bickel et al., 1997; Bodin et al., 2014; Otto and Nichols, 2011). These properties confer to flotillins two major cellular roles: (1) at moderate physiological expression they promote or participate in membrane receptor clustering (Bodin et al., 2014; Guillaume et al., 2013), (2) when upregulated, they induce the formation of PM invaginations that are distinct from caveolae- and clathrin-coated pits (Frick et al., 2007; Glebov et al., 2006). Several cargo molecules, such as Niemann-Pick C1-like 1 protein, CD59 (a glycosylphosphatidylinositol-anchor protein) and amyloid-β peptide precursor are endocytosed through a flotillin-dependent pathway (Aït-Slimane et al., 2009; Ge et al., 2011; Schneider et al., 2008). Recent studies reported that flotillin upregulation in many invasive carcinomas is associated with poor patient survival and high risk of metastasis formation. Upregulation of flotillin promotes cell invasion and metastasis formation, but the molecular mechanisms are not well understood (Berger et al., 2013; Cao et al., 2016; Koh et al., 2016; Pust et al., 2013).

We now demonstrate that flotillins are required for carcinoma and sarcoma cell invasion and that their upregulation, which occurs in many different solid tumor types, promotes cell invasion and ECM degradation through MT1-MMP. We show that flotillins are critical for MT1-MMP targeting to the endolysosomal compartment, which is the MT1-MMP reservoir in cancer cells before its delivery to invadopodia, the major ECM degradation sites. Flotillin upregulation induced RAB5-dependent MT1-MMP endocytosis from the PM to

[1]CRBM, Univ Montpellier, CNRS, France, 1919 Route de Mende, 34293 Montpellier, France. [2]Department of Genetics, Institut Curie, 75005 Paris, France. [3]Cancer Research Institute, Tomsk National Research Medical Center, Tomsk 634050, Russia. [4]Tomsk State University, Tomsk 634050, Russia. [5]Institut für Medizinische Mikrobiologie, Virologie und Hygiene, University Medical Center Eppendorf, Martinistr. 52, 20246 Hamburg, Germany. [6]Cell Dynamics and Compartmentalization Unit, Institut Curie, 75005 Paris, France.
*These authors contributed equally to this work

‡Author for correspondence (cecile.gauthier@crbm.cnrs.fr)

E.R.M., 0000-0002-8504-3805; E.V.D., 0000-0003-0560-9168; V.M.P., 0000-0002-7633-9620

Received 11 April 2018; Accepted 21 July 2018

Journal of Cell Science (2018) 131, jcs218925. doi:10.1242/jcs.218925

this endolysosomal compartment, leading to its polarized secretion, thus favoring ECM degradation and invasion.

RESULTS

Upregulation of flotillins is associated with poor prognosis in patients with carcinoma or sarcoma and promotes cell invasiveness

In several carcinoma types, upregulation of flotillins is associated with poor prognosis (Liu et al., 2015a,b; Pust et al., 2013; Wang et al., 2013; Zhang et al., 2013; Zhu et al., 2013). Here, we confirmed that upregulation of flotillins was significantly associated with poor disease-free survival in a cohort of patients with breast cancer with known long-term outcome, and found that this was true also for sarcoma, using a cohort of patients with rhabdomyosarcoma (RMS) (Bièche et al., 1999; Williamson et al., 2010) (Fig. 1A,B). Specifically, we found a trend toward poorer prognosis in flotillin-overexpressing breast tumors in the whole cohort of 527 breast tumors (Fig. S1A). This observation became significant when comparing in 415 samples the flotillin-1^{high} , flotillin-2^{high} with the flotillin-1^{low}, flotillin-2^{low} subgroups (Fig. 1A). In the 527 breast tumor samples, flotillin co-upregulation was significantly associated with the estrogen, progesterone and *ERBB2* receptor status, molecular subtypes and KI67 expression (Table S1). *FLOT1* and *FLOT2* mRNA expression was positively correlated in breast tumors (r=+0.498, P<10^{-7}) (Fig. S1B). Moreover, we confirmed flotillin-1 and -2 upregulation at the protein level in breast cancer cell lines (Lin et al., 2011; Wang et al., 2013), as previously reported in breast tumor specimens (Lin et al., 2011; Wang et al., 2013), and also in RMS-derived cell lines (Fig. S1C,D). Flotillin protein upregulation was more pronounced in the most invasive RMS cell lines; the alveolar RMS (ARMS) is more aggressive than embryonal RMS (ERMS) (Fig. S1D).

To investigate the role of flotillins in the invasive phenotype of both carcinoma and sarcoma cell lines, we used the invasive MDA-MB-231 (breast cancer) and Rh41 (ARMS) cell lines that exhibit high flotillin expression levels (Fig. S1C-E) (Lin et al., 2011; Wang et al., 2013). We generated stable MDA-MB-231 and Rh41 cell lines that express shRNAs against flotillin-2 (F2 shRNA) or luciferase (CTL shRNA, negative control). As expected, F2 shRNA expression led to a decrease in flotillin protein (Guillaume et al., 2013) (Fig. S1E). Using a three-dimensional (3D) spheroid cell invasion assay with fibrillar type I collagen, we then demonstrated that invasion of MDA-MB-231 and Rh41 F2 shRNA cells was significantly reduced compared with CTL shRNA cells, and that transfection of mCherry-tagged flotillin-2 rescued invasion (Fig. 1C,D). We next asked whether flotillin co-upregulation, as observed in tumors, was sufficient to promote invasive behavior. To this aim, we used non-invasive epithelial (MCF10A) and mesenchymal (C2C12) cell lines with low endogenous flotillin expression levels to generate stable cell lines (MFC10AF1F2 and C2C12F1F2), where flotillins are expressed at levels comparable to those observed in MDA-MB-231 and Rh41 cells (Fig. S1E). Flotillin upregulation increased the invasive potential of MFC10A and C2C12 cells in a 3D spheroid cell invasion assay compared with controls (expressing only mCherry; CTL) (Fig. 1E,F). To investigate the role of flotillins *in vivo*, we used a zebrafish xenograft model and quantified cell dissemination in the tail at day 4-5 after injection of DiI-labeled cells in the perivitelline cavity of fish embryos. Again, we found that compared with control cells, dissemination of MDA-MB-231 F2 shRNA cells was reduced (Fig. 1G), whereas that of C2C12F1F2 cells was increased compared with control cells (Fig. 1H). The number of cells at the time of injection (day 0) and at day 4-5 after injection was comparable in control and flotillin silenced/overexpressing cells (Fig. S2). These data show that flotillins, which are associated with poor prognosis, are required for and promote cancer cell invasion when upregulated.

Flotillin upregulation promotes cell invasion in a proteolytic MT1-MMP-dependent manner

Tumor invasion of collagen-rich ECM is often controlled by matrix metalloproteinases (MMPs) (Friedl and Wolf, 2010; Wolf et al., 2013). Here, we found that invasion of MFC10AF1F2 and C2C12F1F2 cells (3D spheroid cell invasion assay) was reduced by incubation with GM6001, a broad-spectrum MMP inhibitor (Fig. 1I,J). Then, to determine the role of MT1-MMP (MMP14), a key enzyme that degrades intact fibrillar collagen and is involved in tumor cell dissemination and cancer progression (Poincloux et al., 2009; Rowe and Weiss, 2009; Sabeh et al., 2004; Wolf et al., 2007), we analyzed whether flotillin upregulation was implicated in MT1-MMP-dependent gelatin degradation. Using an *in situ* matrix degradation assay, we showed that, as for cancer cell invasion (Fig. 1), flotillin knockdown in MDA-MB-231 and Rh41 cells decreased ECM degradation (Fig. 2A,B), whereas transfection of mCherry-tagged flotillin-2 rescued degradation. Conversely, flotillin upregulation in MCF10A and C2C12 cells increased matrix degradation (Fig. 2C,D), and this effect was impaired by MT1-MMP knockdown (Fig. 2F,G). Moreover, flotillin upregulation in NMuMg cells, which express very low levels of MT1-MMP (Fig. S3A), did not affect ECM degradation (Fig. 2E). Finally, C2C12F1F2 cell dissemination in the zebrafish tail was impaired by knockdown of MT1-MMP expression (Fig. 2H).

However, the total protein and surface-bound levels of MT1-MMP were not affected by flotillin downregulation (F2 shRNA) and upregulation (F1F2) (Fig. S3A,B). Therefore, we assessed the impact of flotillin upregulation on MT1-MMP secretion because MT1-MMP exocytosis at invadopodia is important for local degradation of ECM at these sites in invasive tumor cells (Castro-Castro et al., 2016; Linder et al., 2011). To this aim, we used cells that express MT1-MMP-pHluorin, a protein that is fluorescent only at the extracellular pH of 7.4 (Monteiro et al., 2013), and total internal reflection fluorescence (TIRF) live-imaging to selectively illuminate the ventral PM. We found that flotillin expression level was correlated with MT1-MMP exocytosis. Specifically, the transient dot-like appearance of fluorescent MT1-MMP-pHluorin spots at the ventral PM, reminiscent of exocytic events, was reduced in MDA-MB-231 F2 shRNA cells, and increased in MCF10AF1F2 cells. This effect of flotillin on MT1-MMP exocytosis was not correlated with major changes in the number of invadopodia (Fig. 2I,J). Similarly, we previously showed that flotillin knockdown in macrophages does not affect podosome numbers, but significantly impairs podosomal matrix degradation (Cornfine et al., 2011). Thus, (1) upregulation of flotillins mediates cancer cell invasion and ECM degradation, which strongly relies on MT1-MMP activity, and (2) the expression levels of flotillins influence MT1-MMP exocytosis.

In invasive cells, MT1-MMP endocytosis to the endolysosomal reservoir compartment requires flotillins

Tumor cells hijack MT1-MMP trafficking and develop a recycling circuitry via the endolysosomal compartment that is crucial for MT1-MMP activity (reviewed in Castro-Castro et al., 2016). In invasive MDA-MB-231 and Rh41 cells, we found that flotillin-1 and -2 always colocalized (Fig. S5B), and accumulated with MT1-MMP in RAB7- and CD63-positive vesicles (Fig. 3A and

Journal of Cell Science (2018) 131, jcs218925. doi:10.1242/jcs.218925

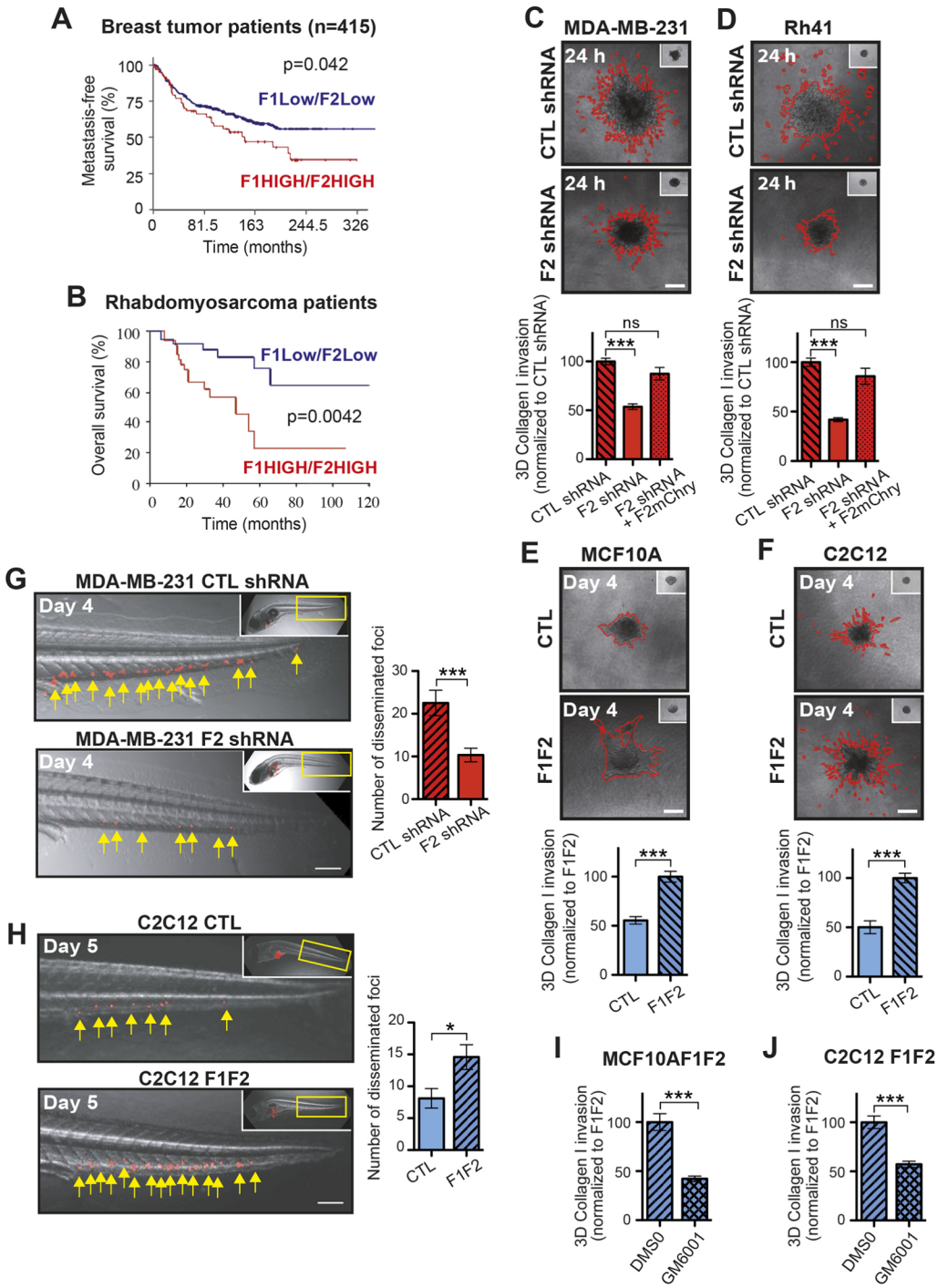

Fig. 1. High flotillin-1 and -2 expression level is correlated with cancer cell invasiveness. (A,B) Kaplan-Meier curves showing metastasis-free survival and overall survival in 415 patients with breast cancer and 101 patients with rhabdomyosarcoma subdivided according to flotillin expression levels in the tumor (high versus low F1 and F2 mRNA levels; optimal cut-offs: F1>1.83 and F2>1.42 for high expression in breast tumors; high>median flotillin expression level in RMS; Spearman rank). (C-F) The invasive breast cancer MDA-MB-231 (C) and invasive RMS Rh41 (D) cell lines that express shRNAs against luciferase (CTL shRNA) or flotillin-2 (F2 shRNA), and the epithelial MCF10A (E) and mesenchymal C2C12 (F) cell lines in which flotillins are upregulated (F1F2) or not (CTL; empty vector) were used for 3D spheroid cell invasion assay. Images taken at the indicated times after embedding in type I collagen are representative of at least 20 spheroids per condition. The insets (top right) show spheroids at day 0 just after embedding. The invasive potential is represented as the mean±s.e.m. of four independent experiments (n=20 spheroids). The histogram also includes analysis of invasion in MDA-MB-231 and Rh41 F2 shRNA cells after rescue of flotillin-2 expression by transfection of a FLOT2-mCherry plasmid (F2mChry). Control cells were used as reference and set at 100%. (G,H) After injection in the zebrafish perivitelline cavity, dissemination of DiI-labeled MDA-MB-231 CTL shRNA and F2 shRNA cells (G) and C2C12 CTL and F1F2 cells (H) in the tail was monitored for 5 days. Confocal images taken at the indicated times after injection are representative of at least 30 injected embryos. Micro-tumor foci are indicated by arrows. Insets show the whole embryos and the yellow box the selected area shown at higher magnification. The histograms (number of disseminated foci per embryo) display the mean±s.e.m. of five independent experiments (n=30 fish). (I,J) 3D collagen invasion assay using MCF10AF1F2 (I) or C2C12F1F2 (J) cells incubated with vehicle alone (DMSO) or with GM6001. The histograms show the mean±s.e.m. of four independent experiments (n=20 spheroids). *P<0.05; ***P<0.001; ns, non-significant (Mann-Whitney test, two-tailed P-value). Scale bars: 150 µm (C-F), 100 µm (G,H).

Journal of Cell Science (2018) 131, jcs218925. doi:10.1242/jcs.218925

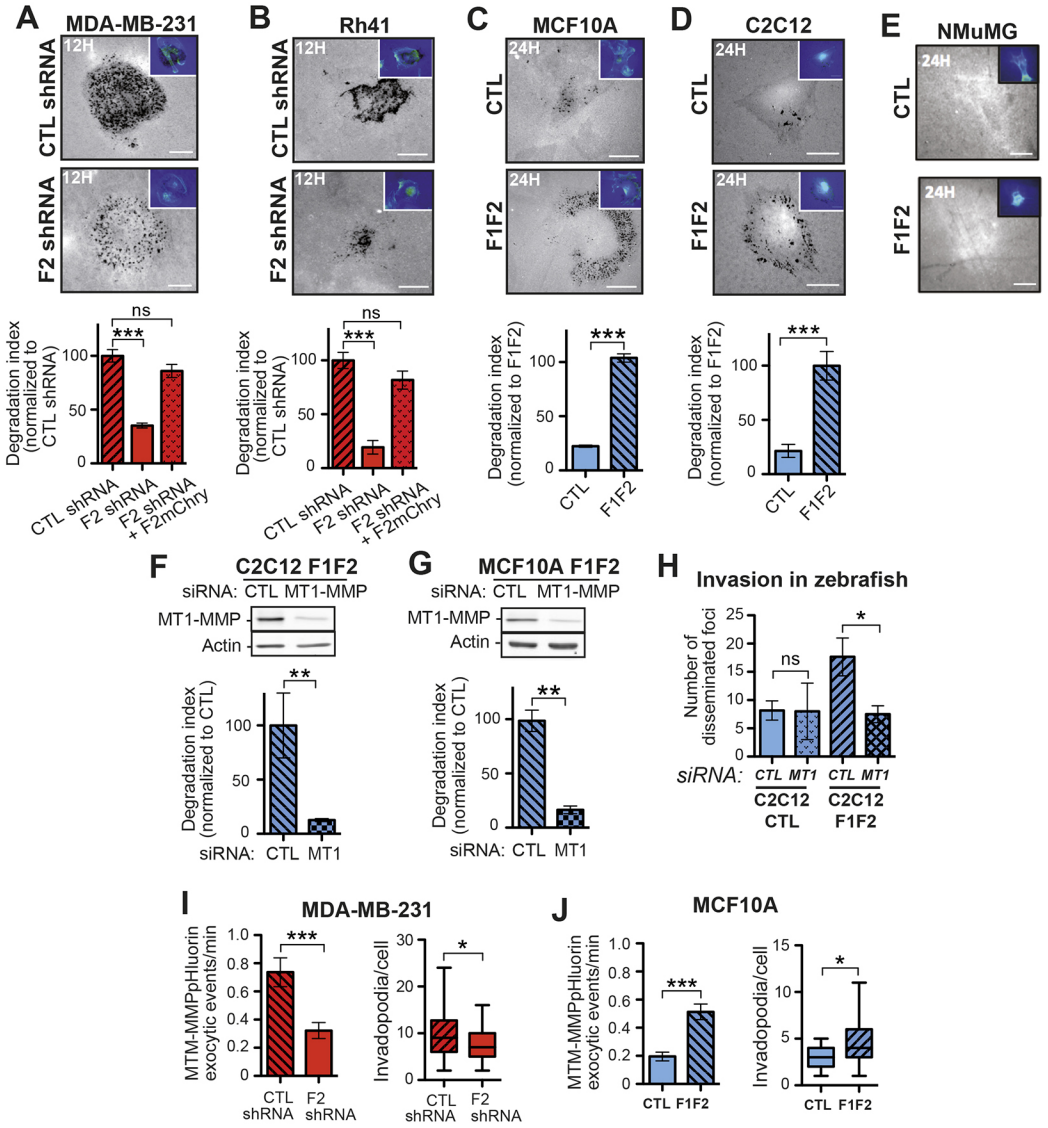

Fig. 2. Flotillin-1 and -2 upregulation induces MT1-MMP-mediated ECM degradation. (A,E) The invasive breast cancer MDA-MB-231, RMS Rh41 cell lines that express shRNAs against luciferase (CTL shRNA) or flotillin-2 (F2 shRNA), and the epithelial MCF10A, mesenchymal C2C12 and NMuMg cell lines in which flotillin-1 and -2 are upregulated (F1F2) or not (CTL; mCherry vector) were used in the FITC-gelatin degradation assay. Shown are representative images of gelatin degradation. Insets show cells visualized by F-actin staining. Histograms display the mean±s.e.m. of four independent experiments (n=240 cells per cell line). The histograms also include the analysis of MDA-MB-231 and Rh41 F2 shRNA cells after rescue of flotillin-2 expression by transfection of a FLOT2-mCherry plasmid (F2mChry). (F,G) Quantification of gelatin degradation by C2C12F1F2 and MCF10AF1F2 cells that express siRNAs against luciferase (CTL) or MT1-MMP. Histograms (lower panels) show the mean±s.e.m. of three independent experiments (n=200 cells per cell line). Western blot analysis (top panels) confirmed the siRNA efficiency. Actin was used as loading control. (H) Histograms (mean±s.e.m. of three independent experiments) show the quantification of disseminated cell foci after injection of C2C12 CTL or F1F2 cells that express siRNAs against luciferase (CTL) or MT1-MMP in the zebrafish perivitelline cavity (n=30 fish). (I,J) Histograms and box plots (mean±s.e.m. of three independent experiments) show the quantification of the MT1-MMP-pHluorin exocytic events in the indicated cell lines from 20 independent movies and the quantification of the number of TKS5-positive invadopodia per cell. *P<0.05; **P<0.01; ***P<0.001; ns, non-significant (Mann-Whitney test, two-tailed P-value). Scale bars: 10 µm.

Fig. S4A). We confirmed that these flotillin- and MT1-MMP-containing vesicles were late/multivesicular endosomes (LE/MVEs), which are described as the endolysosomal MT1-MMP reservoir compartment in cancer cells (Hoshino et al., 2013; Rosse et al., 2014). Indeed, they were positive for RAB7a, LAMP1 and CD63 but not for RAB4, RAB8, RAB11, CD9 and CD81 markers (Fig. 3A and Fig. S4A-D). Moreover, other MMPs such as MMP2, MMP7 and MMP9, did not colocalize with flotillin-2 in intracellular vesicles in MDA-MB-231 cells (Fig. S4E). In addition, confocal time-lapse and TIRF live-imaging analysis of MDA-MB-231 cells confirmed that flotillins and MT1-MMP colocalized in intracellular vesicles that emerge from the PM (Fig. 3B, see white arrow in Movie 1), and also in vesicles addressed to ECM degradation sites (invadopodia) (Fig. 3C and Fig. S4F, Movie 2). We also demonstrated that in MDA-MB-231 cells, MT1-MMP was exocytosed from flotillin-rich intracellular vesicles (Fig. 3D, Movie 3), that we characterized as LE/MVEs/endolysosomes (Fig. 3A and Fig. S4A-D). Patching of the ganglioside GM1 with the CTX-B subunit and using antibodies against CTX-B resulted in co-patching of flotillins and MT1-MMP, supporting the finding that flotillins and MT1-MMP are in the same PM microdomains (Fig. 3E). In addition to their colocalization at vesicles and at the PM in GM1-containing membrane

Journal of Cell Science (2018) 131, jcs218925. doi:10.1242/jcs.218925

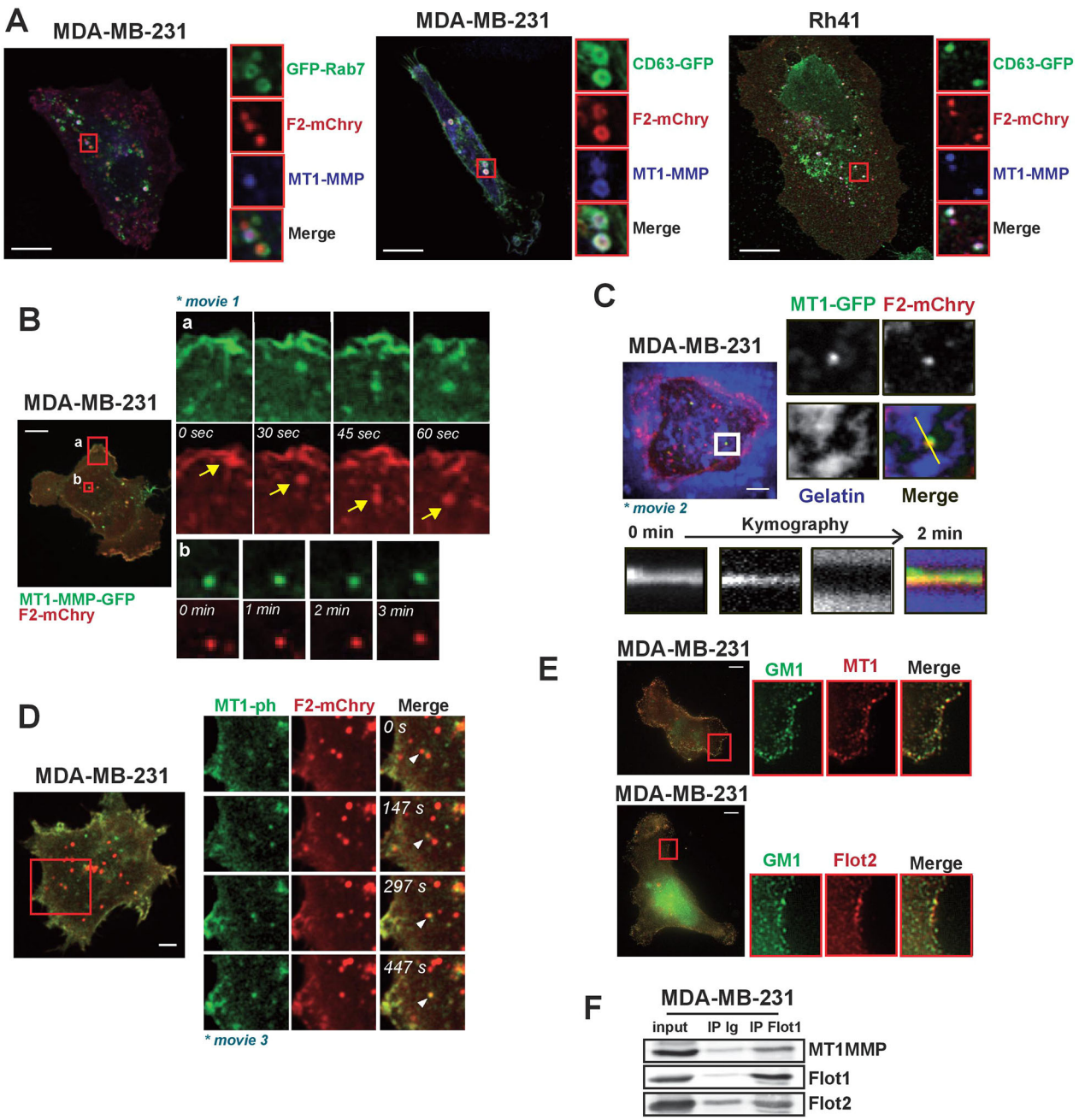

Fig. 3. Flotillins colocalize with MT1-MMP from the PM to the endolysosomal compartment. (A) Confocal micrographs of MDA-MB-231 and Rh41 cells transfected with FLOT2-mCherry (F2-mChry) and GFP-tagged RAB7a or CD63 and incubated with an anti-MT1-MMP antibody to detect endogenous MT1-MMP. The zooms of boxed regions appear on the left side of each image. (B) Still images of a representative time-lapse series (see Movie 1) of one MDA-MB-231 cell that expresses MT1-MMP-GFP and F2-mChry to show F2/MT1-MMP colocalization at the PM (a), at endocytic vesicles forming at the PM (a; arrow) and in intracellular vesicles (b). (C) Still images of one MDA-MB-231 cell that expresses MT1-MMP-GFP and F2-mCherry on Alexa Fluor 633-conjugated fluorescent gelatin (see Movie 2). Kymograph analysis shows the fluorescence intensities in a line scan through the boxed area. MT1-MMP and flotillin-2-containing vesicles are delivered at the degradation area. (D) Spinning disk images of a representative movie (Movie 3) of one MDA-MB-231 cell that expresses MT1-MMP-pHluorin (MT1-ph) and F2-mCherry to visualize MT1-MMP exocytosis at F2-mCherry-positive vesicles (arrowhead). (E) GM1 molecules in MDA-MB-231 cells were labeled with Alexa Fluor 488-conjugated CTX-B subunit and then patched by addition of a secondary antibody. Endogenous MT1-MMP and flotillin-2 were labeled using specific antibodies. Merge images of GM1 and MT1-MMP or GM1 and flotillin-2 are shown. (F) Flotillin-1 was immunoprecipitated from MDA-MB-231 cell lysates. Co-immunoprecipitation of MT1-MMP and flotillin-2 was assessed by immunoblotting. Scale bars: 5 µm.

microdomains, flotillins and MT1-MMP were also co-immunoprecipitated from MDA-MB-231 cell extracts (Fig. 3F), confirming their close association.

As we observed flotillin and MT1-MMP emerging together from the PM into intracellular vesicles (Fig. 3B), we then investigated whether flotillin upregulation influenced MT1-MMP internalization and trafficking to the endolysosomal compartment in MDA-MB-231 cells using an MT1-MMP uptake assay (Remacle et al., 2003). The cell surface level of MT1-MMP was similar in MDA-MB-231 F2 shRNA and control shRNA cells (Fig. 4A,B and Fig.

Journal of Cell Science (2018) 131, jcs218925. doi:10.1242/jcs.218925

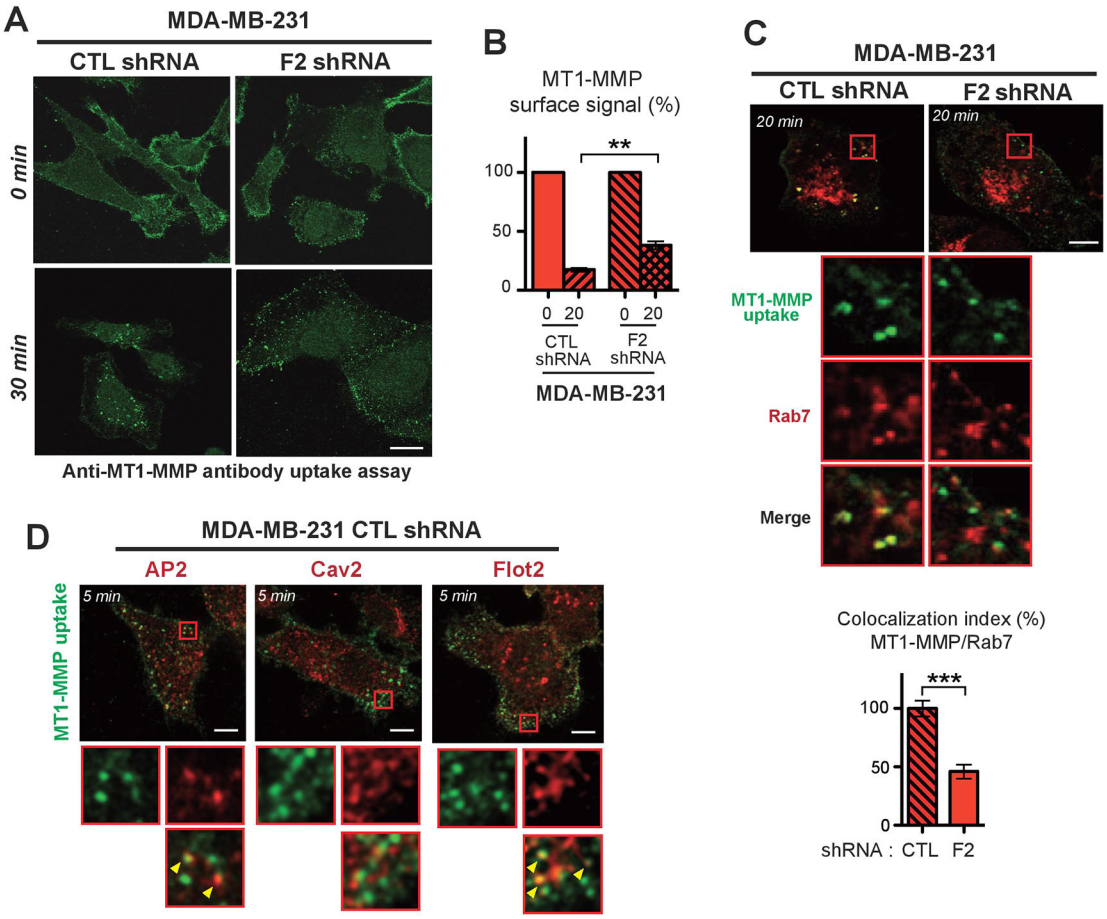

Fig. 4. Flotillins are required for MT1-MMP endocytosis to the endolysosomal compartment. (A-D) MDA-MB-231 cells that express shRNAs against luciferase (CTL shRNA) or flotillin-2 (F2 shRNA) were incubated with an anti-MT1-MMP antibody at 4°C followed by incubation at 37°C for the indicated times to allow MT1-MMP internalization. MT1-MMP distribution was analyzed by immunocytochemistry (A) and MT1-MMP cell surface signal by FACS (B; *n*=50,000 events per cell line). Cells were fixed and permeabilized and incubated with anti-MT1-MMP and anti-RAB7 antibodies to quantify their colocalization (*n*=20 cells) (C). (D) The localization of MT1-MMP, AP2, caveolin-2 and flotillin-2 was analyzed by immunocytochemistry. Arrowheads indicate colocalization. Images are representative of at least five independent experiments. ***P*<0.01; ****P*<0.001 (Mann-Whitney test, two-tailed *P*-values). Scale bars: 5 µm.

S3B). Conversely, MT1-MMP endocytosis was decreased in F2 shRNA cells (Fig. 4A,B). Specifically, MT1-MMP accumulation in endolysosomes was decreased in MDA-MB-231 F2 shRNA cells, without apparent modification of the RAB7 compartment (Fig. 4C). Moreover, in parental MDA-MB-231 cells, MT1-MMP was mainly endocytosed in flotillin-positive vesicles, with almost no colocalization with caveolin (Fig. 4D). We also observed some MT1-MMP-containing vesicles that colocalized with the clathrin adaptor protein 2 (AP2, a clathrin marker), as expected (Fig. 4D) (Remacle et al., 2003). Altogether, these observations strongly suggested that in invasive cancer cells, flotillin upregulation is required for MT1-MMP endocytic traffic from the PM towards endolysosomes.

Flotillin upregulation is associated with its accumulation with MT1-MMP in non-degradative lysosomes

As we observed that the cellular distribution of flotillins strongly differed according to their level of expression, we generated flotillin-knockout C2C12 and MCF10A cells using the CRISPR/Cas9 method to completely abolish their expression (Fig. S1G), and then re-expressed flotillins at low to moderate levels, which corresponds to the endogenous level in non-tumor cells (KO F1/F2 cells). In these cells, flotillins localized to the PM and in few intracellular vesicles (Fig. 5A). Upon re-expression at high levels, flotillins accumulated in intracellular vesicles, as observed in MDA-MB-231 and Rh41 invasive cancer cells where they are endogenously overexpressed (Fig. 5A,B). Flotillin-1 always fully colocalized with flotillin-2 either at the PM or in vesicles (Fig. S5A,B) that we characterized as endolysosomes (Fig. 3A, Fig. S4A-C and Fig. S5C-F). Similarly, analysis of flotillin distribution in invasive breast tumor samples (see Table S2 for description) revealed that flotillin-2 accumulated in intracellular vesicles in malignant cells, whereas it was mainly at the PM in normal cells (acini) (Fig. 5C and Table S2).

Using 3D structured illumination microscopy (3D-SIM), we demonstrated that flotillins and MT1-MMP are in the same PM domains (Fig. 5D). In C2C12F1F2 and MCF10AF1F2 cells, flotillins strongly colocalized with MT1-MMP intracellular vesicles (Fig. 5E), and trafficked together (see Movie 4 for C2C12F1F2 cells), as in invasive cancer cell lines. Moreover, immunohistochemistry analysis of breast tumor sections (Table S2) showed that flotillins and MT1-MMP colocalized in intracellular vesicles of malignant cells in invasive cancer specimens (shown for flotillin-2 in Fig. 5H). In agreement, MT1-MMP and flotillins were co-immunoprecipitated from MCF10AF1F2 cell extracts (Fig. 5F).

The perinuclear vesicles containing flotillins and MT1-MMP were positive for RAB7a and CD63, but not for RAB4, RAB5,

Journal of Cell Science (2018) 131, jcs218925. doi:10.1242/jcs.218925

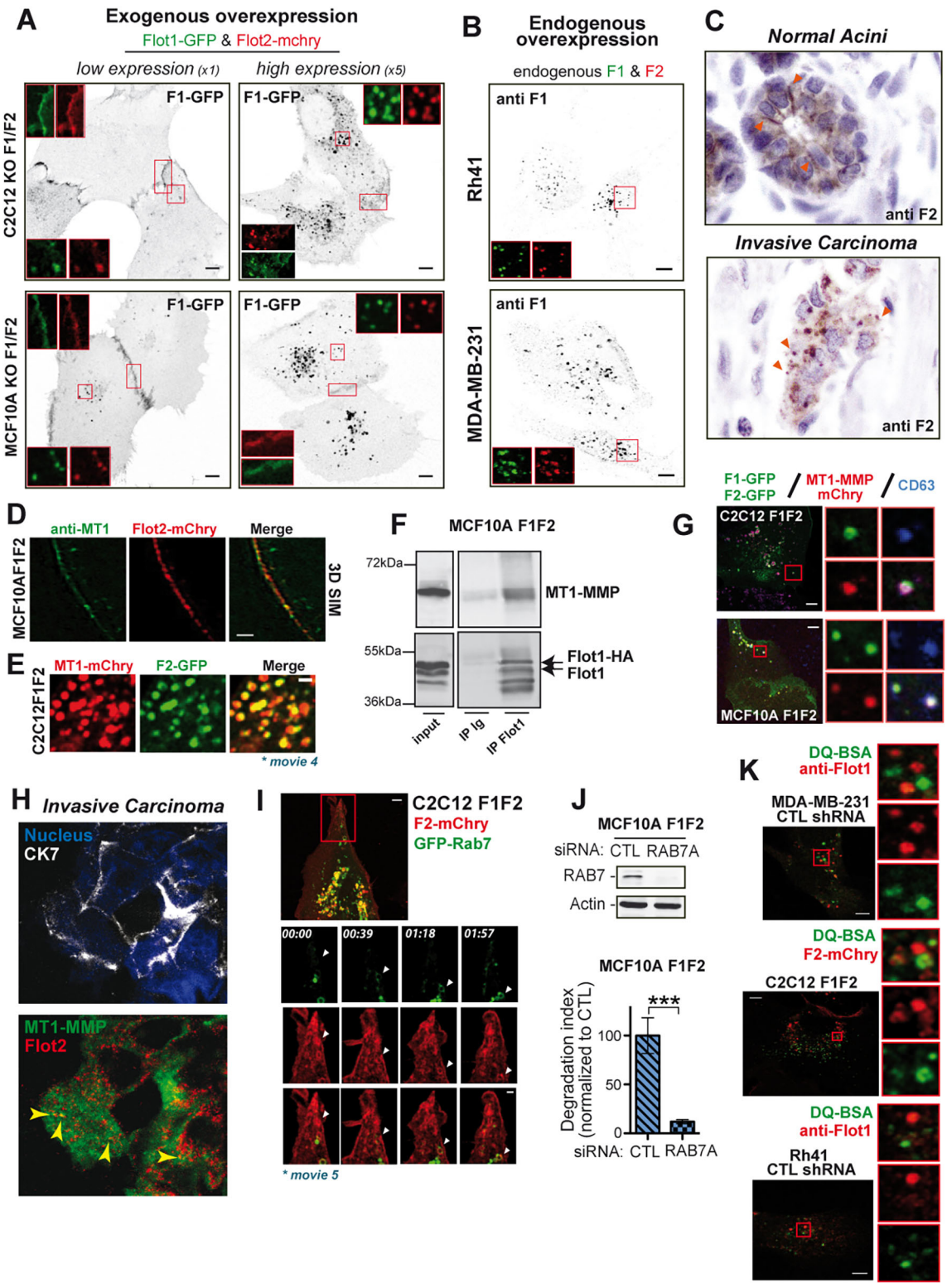

Fig. 5. See next page for legend.

RAB8, RAB11, CD9 and CD81, showing that they co-accumulated in the endolysosomal compartment (Fig. 5G and Fig. S5C-F). Time-lapse analysis revealed that flotillin-rich endocytic vesicles forming at dynamic PM ruffles (red arrow in Movie 5) were rapidly enriched in RAB7, an LE marker (Fig. 5I, and green arrow in Movie 5). Moreover, *RAB7* knockdown in MCF10AF1F2 cells led to a strong decrease in ECM degradation, indicating the functional requirement of this compartment for upregulated flotillin-induced ECM degradation (Fig. 5J).

It is known that proteins can be transported to endolysosomes not only for degradation but also for efficient targeting to the cell surface to drive cell invasion (Rainero and Norman, 2013). To exclude the

Journal of Cell Science (2018) 131, jcs218925. doi:10.1242/jcs.218925

Fig. 5. Upregulated flotillins colocalize with MT1-MMP-containing endocytic carriers trafficking toward the endolysosomal compartment. (A) C2C12 or MCF10A cells in which flotillin-1 and -2 (F1 and F2) were knocked down were transfected with 1× (0.5 µg/2ml=low expression) or 5× (2.5 µg/2ml=high expression) F1-GFP and F2-mCherry expression vectors (KO F1/F2). They were then fixed and flotillin distribution analyzed by confocal microscopy. The inverted contrast image shows the F1-GFP signal. Insets illustrate flotillin-1 and -2 colocalization in the boxed areas. (B) Rh41 and MDA-MB-231 cells were incubated with anti-flotillin-1 and -2 antibodies. The inverted contrast image shows the F1-GFP signal. Insets illustrate flotillin-1 and -2 colocalization. (C) Distribution of flotillin-2 analyzed by immunohistochemistry in breast tumor sections. Flotillin-2 localized mainly to intracellular vesicles in invasive breast cancer specimens (arrows), and to the PM in the adjacent peritumoral breast epithelium tissue (normal acini). Magnification ×400. (D) Analysis of MT1-MMP and flotillin-2-mCherry at the PM in MCF10AF1F2 cells using 3D-SIM. (E) Still images of a representative time-lapse series (see Movie 4) of one C2C12F1F2 cell (GFP-tagged F2) that expresses MT1-MMP-mCherry to illustrate F2/MT1-MMP colocalization in intracellular vesicles. (F) Flotillin-1 was immunoprecipitated from MCF10AF1F2 cell lysates and co-immunoprecipitation of MT1-MMP was assessed by immunoblotting. (G) Detection of CD63 in C2C12 or MCF10A cells that express F1-GFP, F2-GFP and MT1-MMP-mCherry. (H) Immunofluorescence analysis of cytokeratin-7, flotillin-2 and MT1-MMP expression in invasive breast tumor sections (Table S2). Nuclei were stained with Hoechst. Arrows indicate flotillin-2 and MT1-MMP colocalization in intracellular vesicles. (I) C2C12F1F2 cells that express also RAB7A-GFP were monitored by time-lapse confocal imaging (Movie 5). Arrowheads indicate the position of the same vesicle on each frame. (J) FITC-gelatin degradation assay with MCF10AF1F2 cells transfected with anti-RAB7A siRNAs. The histogram shows the mean±s.e.m. of four independent experiments (n=240 cells per condition). ***P<0.001 (Student's t-test, two-tailed P-value). Western blot analysis confirmed the shRNA efficiency. Actin was used as loading control. (K) MDA-MB-231 CTL shRNA, C2C12F1F2 and Rh41 CTL shRNA cells were incubated with DQ-BSA (20 µg/ml) for 4, 3 and 4 h, respectively. Cells were fixed, permeabilized and incubated with an anti-flotillin-1 antibody, as indicated. Images are representative of at least five independent experiments. Scale bars: 5 µm (A-C,G,I,K), 2 µm (D,E,H).

possibility that flotillin-positive endolysosomes were compartments associated with pronounced proteolytic activity, such as lysosomes, we monitored the fluorescence signal generated by lysosomal proteolysis of DQ-BSA, an endocytic probe that becomes fluorescent upon proteolytic cleavage (Fig. 5K). Analysis of the green fluorescent signal from the hydrolyzed DQ-BSA at 3 to 4 h after endocytic uptake did not highlight any significant overlap with that of flotillin-containing vesicles in cells where flotillins are ectopically (C2C12F1F2) or endogenously (MDA-MB-231 and Rh41) upregulated (Fig. 5K). The vesicles with the brightest DQ-BSA signal showed little or no flotillin staining, indicating that flotillin-positive endolysosomes are not associated with major degradation activity.

Flotillin upregulation is sufficient to promote MT1-MMP endocytosis from the PM to its reservoir compartment

As flotillin downregulation in cancer cells affected MT1-MMP endocytosis and impaired trafficking towards endolysosomes, we next asked whether flotillin upregulation was sufficient to directly influence MT1-MMP endocytosis. Using the MT1-MMP uptake assay and analysis of MT1-MMP internalization by immunocytochemistry (Fig. 6A) or flow cytometry (Fig. 6B), we found that flotillin upregulation in MCF10A cells promoted MT1-MMP internalization and also its accumulation in endolysosomes (Fig. 6D). As observed in MDA-MB-231 cells, MT1-MMP colocalized with flotillins at the PM (Fig. 6C, top) and was endocytosed in flotillin-positive vesicles (Fig. 6C, bottom). These data showed that flotillin upregulation is sufficient to induce MT1-MMP endocytosis to endolysosomes, its reservoir compartment.

Flotillin upregulation-mediated MT1-MMP endocytosis and endolysosomal accumulation requires RAB5

As some MT1-MMP-containing vesicles detected outside the perinucelar region were positive for flotillins and also for RAB5 (Fig. S4D), a Rab family protein involved in the control of the proteolytic invasive program (Frittoli et al., 2014), we analysed the role of RAB5 in flotillin upregulation-mediated MT1-MMP endocytosis. Time-lapse analysis of C2C12F1F2 cells revealed that flotillin-rich endocytic vesicles forming at dynamic PM ruffles were RAB5-positive early endosomes that were fusing together (Fig. 7A and yellow arrow in Movie 6). Once fused and enlarged, flotillin-positive vesicles were morphologically similar to the RAB7-positive vesicles shown in Movie 5, and RAB5 was no longer detected (red arrow in Movie 6).

Moreover, RAB5 knockdown in MCF10AF1F2 (ectopic flotillin upregulation) and MDA-MB-231 cells (endogenous flotillin overexpression) using specific siRNAs (Fig. 7B) strongly decreased MT1-MMP endocytosis (Fig. 7C) and its accumulation in the endolysosomal compartment (Fig. 7D), and also decreased ECM degradation (Fig. 7E). Altogether, these data show that RAB5 is required for flotillin-induced MT1-MMP endocytosis towards the endolysosomal compartment and for ECM degradation.

DISCUSSION

In this study, we identified an unprecedented role of flotillins in MT1-MMP trafficking. MT1-MMP is a crucial player in cancer cell invasion because this transmembrane metalloprotease, which can be found at the invasive tumor front, is involved in the breaching of the basement membrane by tumor cells and also in cell invasion through type-I collagen-rich interstitial tissues (Hofmann et al., 2003; Leong et al., 2014; Sabeh et al., 2004; Ueno et al., 1997). MT1-MMP activity is highly regulated, and the control of its intracellular trafficking in cancer cells is of central importance (Castro-Castro et al., 2016). Indeed, alteration of the endocytic machinery can induce cell transformation. Moreover, endocytosis and trafficking of many cargos are misregulated during cancer progression (Sigismund et al., 2012). In cancer cells, MT1-MMP is accumulated in RAB7-positive endolysosomes from which it is transported to invadopodia at the PM (Chevalier et al., 2016; Hoshino et al., 2013; Macpherson et al., 2014; Monteiro et al., 2013; Steffen et al., 2008; Williams and Coppolino, 2011; Yu et al., 2012). However, what drives its accumulation in this endosomal compartment was unknown. We report here that flotillin upregulation plays a major role in MT1-MMP trafficking from the PM to this non-degradative endolysosomal compartment. Flotillin-1 and -2 are upregulated in many invasive carcinoma types, such as melanoma, breast, nasopharyngeal, gastric, cervical, lung, renal and hepatocellular cancer, and this is considered a poor prognostic marker (Bodin et al., 2014; Hazarika et al., 2004; Li et al., 2014; Liu et al., 2015a; Wang et al., 2013; Yan et al., 2014; Zhang et al., 2013, 2014; Zhao et al., 2015; Zhu et al., 2013). We confirmed that flotillin expression is associated with poor prognosis in a large cohort of patients with breast cancer. Moreover, we provided the first demonstration of this correlation also in RMS, a sarcoma of skeletal muscle origin. The only previous study on sarcomas revealed increased *FLOT1* mRNA expression in synovial sarcoma, fibrous histiocytoma and malignant schwannoma (Arkhipova et al., 2014). Using RMS cell lines, we demonstrated higher flotillin-1 and -2 expression in the cell lines derived from ARMS (the most invasive type) than in those derived from ERMS. Altogether, these data suggest that flotillin co-upregulation could be a general mechanism during epithelial and mesenchymal cell

Journal of Cell Science (2018) 131, jcs218925. doi:10.1242/jcs.218925

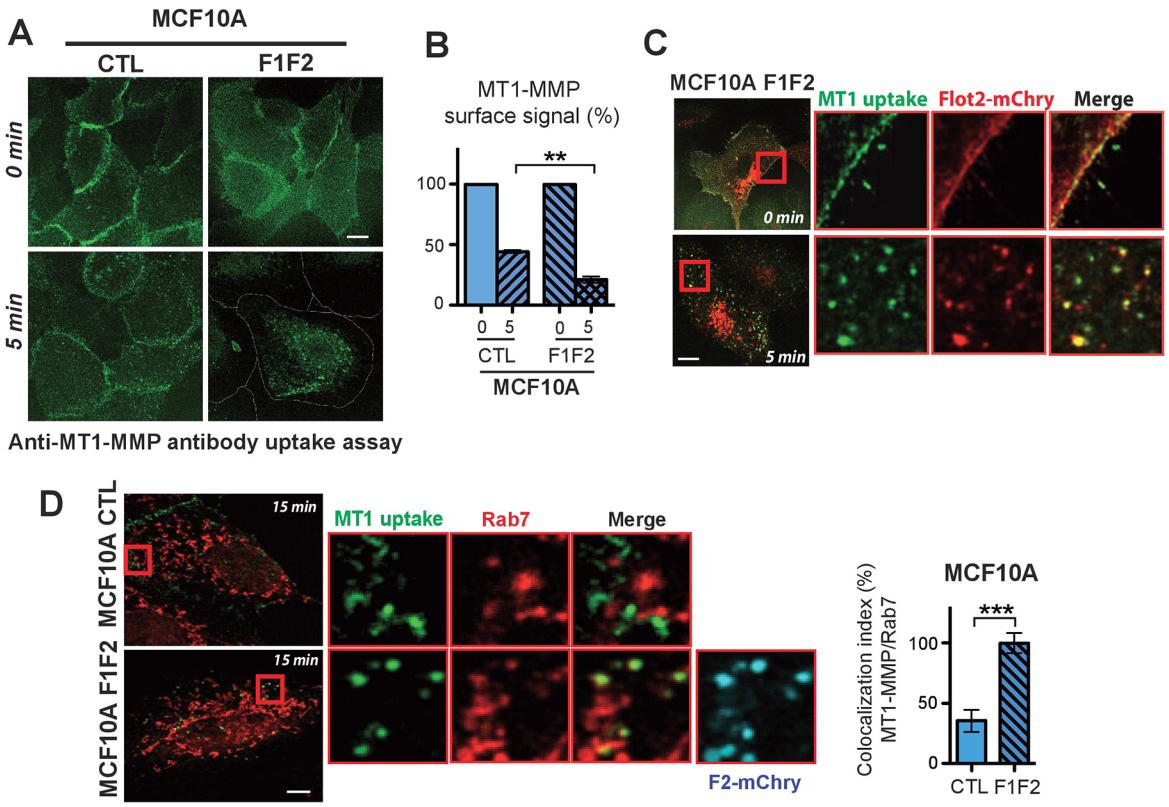

Fig. 6. Upregulated flotillins promote the formation of MT1-MMP-containing endocytic carriers and their movement to the endolysosomal compartment. (A,B) MCF10A CTL and F1F2 cells were incubated with an anti-MT1-MMP antibody at 4°C followed by incubation at 37°C for 5 min. Cells were fixed to allow MT1-MMP detection by immunocytochemistry (A) or by FACS (B) (n=50,000 events per cell line). The histogram shows the mean±s.e.m. of five independent experiments. **P<0.01 (Student's t-test, two-tailed P-value). (C) Confocal micrographs of MCF10A F1F2 cells processed as in A showing flotillin-2 and MT1-MMP colocalization at the PM and in endocytic vesicles. (D) MCF10A CTL and F1F2 cells were processed as in A, fixed for 15 min after incubation at 37°C and incubated with anti-MT1-MMP and anti-RAB7 antibodies. Images are representative of at least five independent experiments. The histogram shows the mean±s.e.m. of four independent experiments (n=20 cells). ***P<0.001 (Mann-Whitney test, two-tailed P-value). Scale bars: 5 µm.

transformation. We then demonstrated for the first time that upregulation of flotillin-1 and -2 is necessary and sufficient to promote breast and RMS cancer cell invasion in 3D collagen matrices and also in the zebrafish tail. This is in agreement with data obtained in a well-established mouse model of mammary tumorigenesis and metastasis showing the crucial role of flotillins in metastasis formation (Berger et al., 2013).

Moreover, flotillin upregulation promoted ECM degradation through the regulation of MT1-MMP endocytosis, an essential process during tissue invasion by tumor cells (Hotary et al., 2006; Leong et al., 2014; Lodillinsky et al., 2016; Rowe and Weiss, 2009). Flotillin localization in cells depends on their expression levels. In invasive cancer cells, where they are upregulated, they accumulate in endolysosomes with MT1-MMP. Progression of carcinoma *in situ* to invasive carcinoma is associated with flotillin translocation from the PM to intracellular vesicles, where they colocalize with MT1-MMP. We then confirmed that this endolysosomal compartment allows preferentially MT1-MMP recycling and not its degradation, thus acting as the reservoir compartment for this metalloprotease in invasive cancer cells (see model in Fig. 8) as previously suggested (Hoshino et al., 2013; Monteiro et al., 2013). We also found that flotillin upregulation allowed the formation of endocytic carriers that contain flotillins and MT1-MMP and that address MT1-MMP to its storage compartment. This is consistent with earlier studies showing that flotillins co-assemble to form membrane microdomains that can induce the formation of GM1-containing PM invaginations and of intracellular vesicles (Frick et al., 2007; Glebov et al., 2006; Lang et al., 1998). Using 3D-SIM, we found that flotillins and MT1-MMP localize in the same PM microdomains, thus explaining MT1-MMP endocytosis into flotillin-rich PM invaginations. Moreover, GM1 patching with the CTX-B subunit resulted in co-patching of flotillins and MT1-MMP, again supporting the finding that flotillins and MT1-MMP are in the same PM microdomains (Fig. 3E). It was previously demonstrated that these cholesterol-rich PM microdomains contain MT1-MMP (Annabi et al., 2001; Galvez, 2003). It was proposed that in HT1080 fibrosarcoma cells, MT1-MMP endocytosis is controlled by several clathrin-dependent and -independent endocytic pathways (Baldassarre et al., 2015; Remacle et al., 2003). Although caveolae might interfere with MT1-MMP-dependent ECM degradation in MDA-MB-231 cells (Yamaguchi et al., 2009), their direct role in MT1-MMP uptake is unlikely, and they might be involved in membrane and invadopodia organization and in sensing the mechanical stress encountered by tumor cells during invasion (Parton and del Pozo, 2013; Yamaguchi et al., 2009). Indeed, we never observed caveolin and MT1-MMP colocalization in MDA-MB-231 cells during MT1-MMP endocytosis from the PM to endolysosomes. Conversely, we demonstrated that flotillin upregulation-induced endocytosis is the major clathrin-independent pathway for MT1-MMP internalization from the cell surface to the endolysosomal compartment.

Some members of the Rab family of small GTPases, key regulators of membrane trafficking, are involved in the regulation of MT1-MMP

Journal of Cell Science (2018) 131, jcs218925. doi:10.1242/jcs.218925

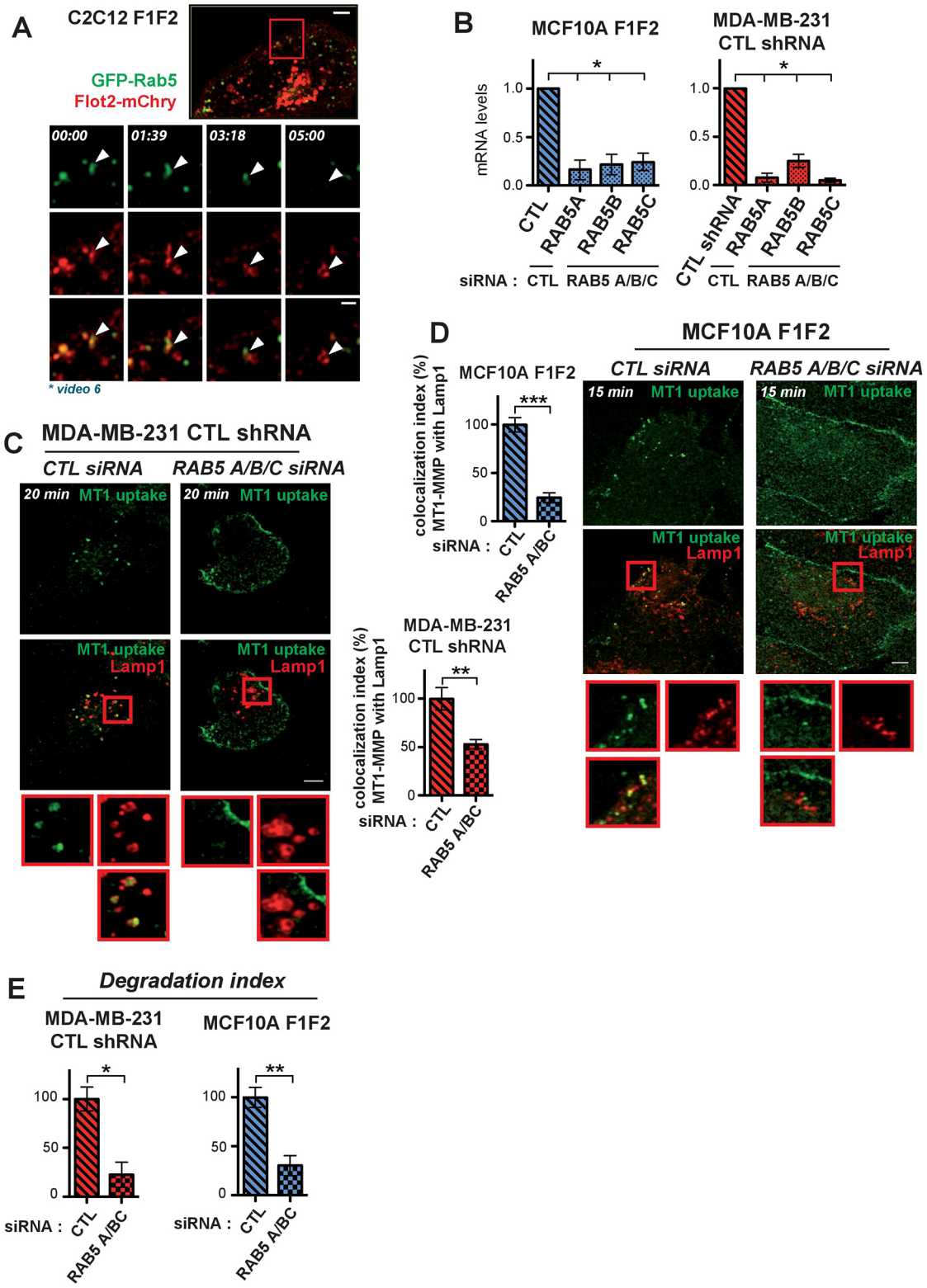

Fig. 7. See next page for legend.

endo-exocytic recycling pathways (Bravo-Cordero et al., 2007; Frittoli et al., 2014; Kajiho et al., 2016; Macpherson et al., 2014; Remacle et al., 2003; Steffen et al., 2008; Williams and Coppolino, 2011). Our data highlight a role for upregulated flotillins in MT1-MMP endocytosis from early to endolysosomes before PM delivery at degradation sites, which corresponds to the main trafficking pathway in cancer cells. Consistently, we demonstrated that flotillin upregulation-induced matrix degradation in normal cells is abrogated upon knockdown of RAB5 or RAB7, two Rab proteins with major function during tumorigenesis (Alonso-Curbelo et al., 2014; Frittoli et al., 2014). In invasive MDA-MB-231 cancer cells, in which flotillins are upregulated, RAB5 knockdown impaired matrix

Journal of Cell Science (2018) 131, jcs218925. doi:10.1242/jcs.218925

Fig. 7. MT1-MMP endocytosis promoted by flotillin upregulation is dependent on RAB5. (A) C2C12F1F2 myoblasts were transfected with GFP-RAB5 and monitored by time-lapse confocal imaging (Movie 6). Arrowheads indicate the position of the same vesicle on each frame. (B) MCF10AF1F2 and MDA-MB-231 cells were transfected with siRNAs against luciferase (CTL siRNA) or *RAB5a*/*b*/*c* and siRNA efficacy assessed by RT-qPCR. The histogram shows the mean±s.e.m. of four independent experiments. (C) MDA-MB-231 transfected with siRNAs against luciferase (CTL siRNA) or *RAB5a*/*b*/*c* were incubated with an anti-MT1-MMP antibody at 4°C followed by incubation at 37°C for 20 min. Cells were fixed and permeabilized to assess MT1-MMP and LAMP1 localization. The histogram (mean±s.e.m. of four independent experiments, *n*=20 cells) shows MT1-MMP and LAMP1 colocalization index. (D) MCF10AF1F2 cells transfected with siRNAs against luciferase (CTL siRNA) or *RAB5a*/*b*/*c* were incubated with an anti-MT1-MMP antibody at 4°C followed by incubation at 37°C for 15 min. Cells were fixed to allow MT1-MMP and LAMP1 detection by immunocytochemistry. The histogram (mean±s.e.m. of four independent experiments, *n*=20 cells) shows the MT1-MMP and LAMP1 colocalization index. (E) Histogram (mean±s.e.m. of three independent experiments, *n*=200 cells) shows the quantification of FITC-gelatin degradation by MCF10AF1F2 or MDA-MB-231 cells transfected with siRNAs against luciferase (CTL siRNA) or *RAB5a*/*b*/*c*. **P*<0.05, ***P*<0.01, ****P*<0.001 determined with the Mann-Whitney test, two-tailed *P*-values (B-D) and the Student's *t*-test, two-tailed *P*-values (E). Scale bars: 5 µm (insets in A, 2 µm).

degradation, as previously shown upon RAB7 knockdown (Kajiho et al., 2016).

Flotillin-mediated MT1-MMP targeting to endolysosomal compartments is crucial for its subsequent efficient recycling and exocytosis at degradation sites from this storage compartment. This endolysosomal recycling route has emerged as a key process in the delivery at the cell surface of cargos such as integrins or their ligands, to regulate cell migration and tumorigenesis (Dozynkiewicz et al., 2012; Rainero and Norman, 2013; Sung et al., 2015). This flotillin-containing endolysosomal compartment participates in MT1-MMP recycling, but not in its degradation. Indeed, the flotillin- and MT1-MMP-containing vesicles were not associated with major proteolytic activity, measured with the DQ-BSA probe, and MT1-MMP protein level was not modified in cells where flotillins were knocked down or upregulated. This shows that MT1-MMP is sorted in this recycling non-degradative endolysosomal compartment, named LE/MVEs by Hoshino et al. (2013) and Rosse et al. (2014), to allow its exocytosis. This is in agreement with data showing MT1-MMP-polarized trafficking from the RAB7-positive endolysosomal vesicles to sites of cell-matrix adhesion (Macpherson et al., 2014; Steffen et al., 2008; Williams and Coppolino, 2011; Yu et al., 2012), and with the release of internalized MT1-MMP in the extracellular space (Uekita et al., 2001). The absence of a detectable change in MT1-MMP cell surface level upon flotillin upregulation or knockdown suggests the endocytosis of a small, but crucial fraction of MT1-MMP and/or the existence of a very fast recycling process. This trafficking process allows the efficient concentration of MT1-MMP from its homogenous PM distribution to degradation sites, thus promoting its activity. This is achieved by MT1-MMP targeting from the PM to endolysosomes that allows its polarized delivery and concentration at degradation sites. This study provides evidence for a crucial gain-of-function role of flotillins, which are upregulated in many carcinomas and sarcomas, during cancer cell invasion and ECM degradation and reveals a new opportunity for diagnostic and/or therapeutic interventions.

MATERIALS AND METHODS

Cell lines

All cell lines were authenticated and tested for contamination. The MCF10A non-tumorigenic mammary epithelial cell line (American Type Culture Collection, ATCC CRL-10317) was grown in DMEM/HAM F-12 medium supplemented with 5% horse serum (Gibco, Thermo), 10 µg/ml insulin, 20 ng/ml EGF, 0.5 µg/ml hydrocortisone and 100 ng/ml cholera toxin. C2C12 mouse myoblasts (ATCC CRL-1772) and Rh41 cells were grown in DMEM supplemented with 10% fetal calf serum (FCS) (Biowest, Eurobio). The NMuMG mouse mammary epithelial cell line (ATCC CRL-1636) was grown in DMEM supplemented with 10% FCS (Biowest, Eurobio) and 10 µg/ml insulin. The human breast adenocarcinoma cell line MDA-MB-231 (ATCC HTB-26) and all ERMS and ARMS cell lines (Thuault et al., 2013) were grown in DMEM with 10% FCS (Biowest, Eurobio). Retrovirus production in Phoenix cells (Garry Nolan, Stanford University, CA, USA), infection and selection were performed as described (Fortier et al., 2008). Cells were grown continuously in 1 µg/ml puromycin and 200 µg/ml hygromycin.

Plasmid constructs

The retroviral plasmid containing flotillin-2 tagged with mCherry was made by subcloning the human *FLOT2* sequence in the pBabe-puro-mCherry vector using the *Xho*I and *Eco*RI restriction sites. The retroviral plasmid encoding HA-tagged flotillin-1 was obtained by subcloning the FLOT1-HA sequence from the previously described phCMV3-Flot1-HA plasmid (Guillaume et al., 2013) into pMSCV-hygro between the *Xho*I and *Hpa*I sites. The retroviral plasmid encoding GFP-tagged flotillin-2 was made by subcloning the FLOT2-GFP sequence from the previously used peGFP-N1-Flot2 construct (Guillaume et al., 2013) into pMSCV-puro between the *Nco*I and *Not*I sites. The pBabe-puro-mCherry vector was obtained by subcloning mCherry from pmCherry-N1 into pBabe-puro between the *Age*I and *Bgl*II sites. The peGFP-N1-MT1-MMP plasmid was a gift from Maria Montoya (CNIC, Madrid, Spain). The pCDNA3.1 MT1-MMP mCherry and MT1-MMP-pHluorin plasmids were gifts from Philippe Chavrier (Curie Institute, Paris, France) (Rosse et al., 2014). MMP2-GFP was a gift from Santiago Rivera (Université de Marseille, France). The pcDNA3-MMP7-GFP plasmid was purchased from Addgene, and MMP9-GFP was a gift from Rene Harrison (University of Toronto, Canada). GFP-RAB8 was a gift from Mariane Martin (Université de Montpellier, France) (Chevalier et al., 2016). The CD63-GFP encoding plasmid was a gift from Alissa Weaver (Vanderbilt University, Nashville, USA) (Sung et al., 2015).

RNA interference

The pSIREN-RetroQ-Flot2-shRNA (targeting both human and murine *Flot2*) and pSIREN-RetroQ-Luciferase shRNA vectors were previously described (Guillaume et al., 2013). For RNA-mediated interference experiments, cells were transfected using Interferin (Polyplus Transfection) with siRNA oligonucleotide duplexes (Eurogentec, Belgium). The sequences of the siRNA duplexes are listed in Table S3. Luciferase shRNA was used as a control (Fortier et al., 2008).

CRISPR/Cas9 knockout of flotillin-1 and flotillin-2

The guide RNAs were cloned as previously described (Ran et al., 2013) into the pSpCas9(BB)-2A-GFP (PX458) vector (Addgene plasmid #48138 deposited by Feng Zhang; Ran et al., 2013). The guide RNA plasmids were transiently transfected into C2C12 or MCF10A cells to knockout mouse *Flot1* and *Flot2*, and human *FLOT1* and *FLOT2*.

Zebrafish tumor model

Zebrafish (*Danio rerio*) AB lines were raised and kept in standard laboratory conditions, according to the European Union guidelines for the handling of laboratory animals (http://ec.europa.eu/environment/chemicals/lab_animals/home_en.htm). Animal studies were approved by the Direction Sanitaire et Vétérinaire de l'Hérault and the Comité d'Ethique pour l'Expérimentation Animale under reference B-34-172-39. At 24 h post-fertilization, fish embryos were incubated with water containing phenylthiourea to prevent pigmentation. At 48 h post-fertilization, zebrafish embryos were dechorionated and anesthetized with 0.04 mg/ml tricaine (Sigma). 500 DiI-labeled tumor cells were injected into the perivitelline space using an Eppendorf microinjector. After injection, embryos were transferred into housing water, and tumor cell invasion was monitored using a fluorescent microscope (Leica SP5) for 5 days. Cell invasion was measured by automated

Journal of Cell Science (2018) 131, jcs218925. doi:10.1242/jcs.218925

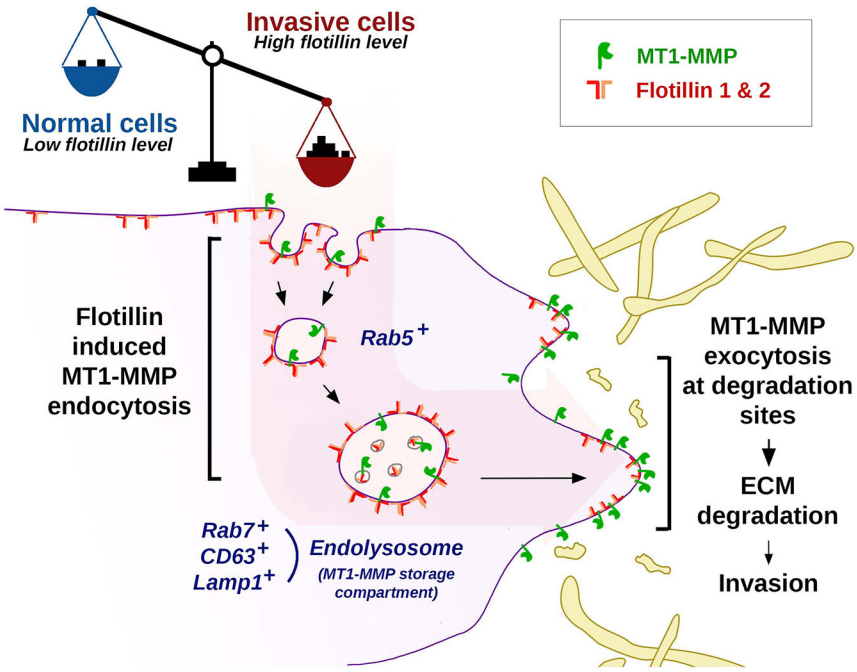

Fig. 8. Model for the role of flotillins in MT1-MMP endolysosomal recycling. Flotillin-1 and -2 upregulation (in invasive tumor cells or after ectopic expression) promotes the formation of MT1-MMP-containing RAB5-positive early endosomes that fuse together and quickly undergo early to late endosomal maturation and become enriched in RAB7. This MT1-MMP-containing endolysosomal compartment promoted by flotillin upregulation does not show major degradation activity and corresponds to the MT1-MMP reservoir compartment from which MT1-MMP is subsequently efficiently recycled and exocytosed at degradation sites.

quantification of the number of DiI-labeled cells in the zebrafish tail using ImageJ. Embryos were dissociated and fluorescent cells counted by FACS.

Antibodies and reagents

Mouse antibodies used were against actin (1:5000, A5441, Sigma), flotillin-1 (1:1000, 610820, BD Biosciences), flotillin-2 (1:100, 610383, BD Biosciences), MT1-MMP (1:400, 3328, Millipore), Rab7 (1:400, 50533, Abcam), LAMP1 (1:500, 555798, BD Biosciences), caveolin 2 (1:100, 610684, BD Biosciences), AP2 (1:100, 610501, BD Biosciences), ER (IR657 clone 1D5, ready-to-use, Dako), PR (IR068 clone PgR636, ready-to-use, Dako), Ki-67 (M306 clone SP6, ready-to-use, Spring Bioscience), CD63 (1:50, clone R5G2, MBL), CD81(1:50, D131-4, clone R5G2, MBL) and CD9 (1:50, D131-3, MBL).

Rabbit antibodies against MT1-MMP (1:1000 WB, 1:50 Uptake, ab51074, Abcam), flotillin-1 (1:100 IF, 1:50 IHC, F1180, Sigma), flotillin-2 (1:100 IF, 1:1000 WB, 3436, Cell Signaling Technology), RAB7 (1:1000, 9367, Cell Signaling Technology), Tks5 (1:100, sc30122, Santa Cruz), HER2 (1:800, A0485, Dako), HA (1:100, 71-5500, Thermo), HER2 (1:800, A0485, Dako) and actin (1:5000, A2066, Sigma) were also used.

Alexa Fluor 350-, 405-, 488-, 546-, 633- and Dylight 680/800-conjugated secondary antibodies were from Thermo Scientific. Alexa Fluor 350-conjugated phalloidin (A-22281), DQ-Green BSA (D12050) and Cell Tracker CM-DiI Dye (C7000) were from Thermo Scientific and GM6001 was from Calbiochem (364206).

MT1-MMP uptake experiments

Cells were seeded on 12 mm sterile round glass coverslips and grown to 60-70% confluence. They were then washed twice with PBS at 4°C. After 10 min incubation at 4°C in serum-free medium, cells were incubated at 4°C in serum-free medium containing 10 µg/ml anti-MT1-MMP rabbit antibody (Abcam) for 30 min. Cells were extensively washed with ice-cold PBS to remove unbound antibodies and surface-bound antibodies were internalized by incubating cells at 37°C in serum-free medium for the indicated time points. Cells were then fixed and permeabilized, and the internalized primary antibody molecules were detected using the appropriate fluorescent secondary antibody. Samples were then processed as described in the Immunofluorescence and image acquisition section.

3D spheroid cell invasion assays

Spheroids were prepared as described (Thuault et al., 2013). GM6001 (30 µM) was added to the coating, the embedding solution and the medium layered on top of the collagen. After embedding, spheroids were monitored by time-lapse imaging, and phase-contrast photographs were taken over 5 days. The invaded area was measured using ImageJ (http://dev.mri.cnrs.fr/projects/imagej-macros/wiki/Phase_Contrast_Cell_Analysis_Tool_%28Trainable_WEKA_Segmentation%29). Control conditions were set at 100%. Data are the mean±s.e.m. of at least four independent experiments in which at least five spheroids were embedded per experimental condition.

Degradation assays

Coverslips were coated with 50 µg ml^{-1} poly-D-lysine followed by 0.5% glutaraldehyde, and then inverted on a 20 µl drop of 10:1 mixture of gelatin/Oregon Green 488-conjugated gelatin (Life Technologies). The gelatin matrix was then quenched with 5 mg/ml sodium borohydride and rehydrated in complete growth medium before use. Cells were plated on fluorescent gelatin for 12 h (MDA-MB-231 and Rh41 cells) or 24 h (C2C12 and MCF10A cells), and then fixed in 3.2% PFA. Samples were then processed as described in the Immunofluorescence and image acquisition section.

MT1-MMP-pHluorin exocytosis experiment

Cells that express MT1-MMP-pHluorin were plated on glass-bottom dishes (Ibidi) coated with non-fluorescent cross-linked gelatin. Cells were imaged by TIRF microscopy (1 image/20 s). The number of exocytic events of MT1-MMP-phLuorin (i.e. GFP flashes) was counted per minute and per cell. TIRF images were acquired using an inverted Nikon microscope and a 100×/1.49 oil objective controlled using the Metamorph software.

Immunofluorescence and image acquisition

Cells were fixed in 3.2% paraformaldehyde (in phosphate-buffered saline, PBS) for 15 min, followed by a 2 min permeabilization with 0.1% Triton X-100 (in PBS) and saturation with 2% BSA (in PBS). For CD9, CD63 and CD81 detection, cells were permeabilized using 0.1% saponin. Cells were incubated with primary and secondary antibodies in PBS containing 2% BSA. Ganglioside GM1 patching was performed as described (Causeret et al., 2005) using cholera toxin subunit-β conjugated to Alexa Fluor 488 (1:1000, Thermo, C34775) and an anti-cholera toxin subunit-β antibody (1:1000, Abcam, ab34992).

Confocal images were acquired using a Confocal Leica SP5-SMD microscope and a Leica 63×/1.4 oil HCX PL APO CS objective controlled using the Leica LAS AF software. Co-localization data originated from multichannel fluorescence stacks collected using a Leica SP5 microscope. For each stack, a single value of the Pearson's coefficient (ranging between −1 and

Journal of Cell Science (2018) 131, jcs218925. doi:10.1242/jcs.218925

1) was measured at the cell-cell junction imposing a threshold value calculated based on the algorithms by Costes et al. (2004) for green and red channels using the 'co-localization analysis' section of Imaris (Bitplane). For 3D-SIM, cells were treated and imaged as described (Guillaume et al., 2013).

Time-lapse imaging

Images were acquired using a confocal microscope (Confocal Leica SP5-SMD) equipped with thermal, CO_2 and humidity controllers and a Leica 63×/1.4 oil HCX PL APO CS objective and captured with a hybrid detector (Leica HyD) controlled using the Leica LAS AF software. Images were taken every 5 s.

Immunoprecipitation

The monoclonal anti-flotillin-1 (1 µg, BD Biosciences, 610820) antibody was incubated with Protein-G Sepharose beads at room temperature for 1 h. After washing, 750 µg of protein extract was added at 4°C for 2 h. Immunoprecipitates were analyzed by immunoblotting.

Cell surface biotinylation

The presence of MT1-MMP at the cell surface was analyzed as described previously (Charrasse et al., 2006). Quantification of at least three independent experiments was performed using the Odyssey system (LI-COR Biosciences).

Microarray analysis

The described HG-U133plus2.0 Affymetrix microarray data for RMS tumor samples were used for gene expression analyses (Williamson et al., 2010). Low and high expression were lower and higher than the median expression level, respectively.

RT-qPCR analysis of breast tumor samples

Flotillin mRNA level in tumor samples from the cohort of patients with breast cancer were analyzed as described (Rosse et al., 2014). Values for *FLOT1*>1.83 and *FLOT2*>1.42 were considered to represent high mRNA expression levels in tumor samples.

Patients and specimens

Patients (n=10) with breast carcinoma treated at the Cancer Research Institute, Tomsk NRMC (Tomsk, Russia) were included (Table S2). The histological type was defined according to the World Health Organization recommendations (Lakhani et al., 2012). Tumor grade was determined using the Bloom and Richardson system (Bloom and Richardson, 1957). Estrogen receptor (ER) and progesterone receptor (PR) immunostaining were scored using the HSCORE method (Kinsel et al., 1989). HER2 expression was analyzed by immunohistochemistry and calculated on a scale 0-3+, according to the ASCO/CAP guidelines (Wolff et al., 2007). Ki-67 expression was calculated as the percentage of Ki-67-positive cells relative to all cells. Molecular subtypes were categorized using the ER, PR, HER2 and Ki-67 status of the primary tumor according to the St Gallen recommendations (Coates et al., 2015): luminal A (ER^+ and/or PR^+, $HER2^-$ and Ki-67<20%), luminal B (ER^+ and/or PR^+, $HER2^{+/-}$ and Ki-67≥20%), $HER2^+$ (ER^- and PR^-, $HER2^+$) and triple-negative (ER^-, PR^-, $HER2^-$).

Frozen and formalin-fixed, paraffin-embedded (FFPE) tumor tissue specimens obtained during surgery were used for immunohistochemical and immunofluorescence analyses. The procedures followed in this study were in accordance with the Helsinki Declaration (1964, amended in 1975 and 1983). This study was approved by the institutional review board; all patients signed an informed consent for voluntary participation.

Clinicopathological characteristics were noted of the patients who gave the breast cancer samples used for the expression analysis in Table S2. #7425: 35-year-old woman, multifocal invasive carcinoma (right side), T2N1M0 (T1N0M0 after surgery), grade 2, ER+ (8), PR+ (7), HER2 (2+), Ki-67-positive cells (40%), luminal B. Six courses of neoadjuvant chemotherapy, effect – intermediate residual disease (RCB-II). Lymph node-negative (0 metastasis in 12 lymph nodes); #20265: 47-year-old woman, invasive carcinoma (right side), T2N1M0, grade 2, ER+ (7), PR+ (7), HER2 (2+), Ki-67-positive cells (25%), luminal B. No neoadjuvant chemotherapy. Lymph node-positive (14 metastases in 21 lymph nodes); #4384: 50-year-old woman, multifocal invasive carcinoma (right side) with micropapillary component, T2N1M0, grade 2, ER+ (7), PR+ (7), HER2 (1+), Ki-67-positive cells (45%), luminal B. Two courses of neoadjuvant chemotherapy without effect (extensive residual disease, RCB-III). Lymph node-positive (1 metastasis in 12 lymph nodes); #3807: 60-year-old woman, invasive carcinoma, T1N0M0, grade 2, synchronous bilateral, ER+ 7 (5+2), PR+ 4 (2+2), HER2 (2+), Ki-67-positive cells (30%), luminal B. No neoadjuvant chemotherapy. Lymph node-negative (0 metastasis in 6 lymph nodes); #25224: 60-year-old woman, invasive carcinoma, T2N1M0, grade 2, ER+ 8 (5+3), PR+ 0, Her2 1+, Ki-67 30%, luminal B. Without neoadjuvant chemotherapy. Lymph node-positive (2 metastasis in 12 lymph nodes); #20463: 41-year-old woman, invasive carcinoma (left side), T2N0M0, grade 2, ER−, PR−, HER2 (3+), Ki-67-positive cells (51%). Six courses of neoadjuvant chemotherapy, effect: minimal residual disease (RCB-I). Lymph node-negative (0 metastasis in 14 lymph nodes); #7655: 74-year-old woman, invasive carcinoma (left side), T2N0M0, grade 3, ER−, PR−, HER2−, Ki-67-positive cells (50%), triple negative. No neoadjuvant chemotherapy. Lymph node-positive (1 metastasis in 8 lymph nodes).

Immunohistochemical staining of tumor samples

Immunohistochemical staining was used for the standard scorings (ER, PR, HER2 and Ki-67) and to assess flotillin-1 and -2, MT1-MMP and cytokeratin 7 expression. Primary mouse antibodies were against ER (IR657, clone 1D5, ready-to-use, Dako, Denmark), PR (IR068, clone PgR636, ready-to-use, Dako, Denmark), Ki-67 (M306, clone SP6, ready-to-use, Spring Bioscience). Primary rabbit antibodies against HER2 (A0485, 1:800, Dako, Denmark), flotillin-1 (F1180, 1:50, Sigma) and flotillin-2 (3436, 1:100, Cell Signaling Technology) were also used. Immunohistochemical staining was performed as previously described (Zavyalova et al., 2013).

Immunofluorescence staining of tumor samples

Seven-µm-thick FFPE tumor sections were deparaffinized, rehydrated, processed for heat-induced epitope retrieval in PT Link (Dako, Denmark) with EDTA buffer (pH 8.0), and blocked with 3% bovine serum albumin (Amresco, USA) in PBS. Sections were incubated with primary antibodies against cytokeratin 7 (CK7, clone N-20, 1:50, Santa Cruz), flotillin-1 (F1180, 1:100, Sigma), flotillin-2 (3436, 1:100, Cell Signaling Technology) and MT1-MMP (MAB3328, 1:400, Millipore). The following secondary antibodies were used: donkey anti-mouse Alexa Fluor 488 (Abcam, USA), donkey anti-rabbit Cy 3 (Abcam, USA), and donkey anti-goat Alexa Fluor 647 (Abcam, USA). Vectashield mounting medium (Vector Laboratories, USA) containing the DAPI nuclear staining was used to mount the sections. Samples were analyzed using a LSM 780 NLO confocal microscope (Carl Zeiss, Germany).

Statistical analysis

All statistical analyses were performed using SPSS version 22, and graphs were generated with Prism GraphPad version 5. All data were first tested for normality using the Kolmogorov-Smirnov normality test. For experiments with n>30, the Student's t-test was used to identify significant differences between experimental conditions. For experiments with n<30, the non-parametric Mann-Whitney U-test was used. The n value and number of independent experiments are listed in the figure legends. At least three independent experiments were performed.

Acknowledgements

We thank Clément Chevalier, Christine Bénistant, Eric Rubistein and Clothilde Théry for discussions, Marie Morille for Nanosigh experiments, Nabila Elarouci and Aurélien De Reynies from the Ligue Nationale contre le Cancer (Carte d'identité des tumeurs) for transcriptomic analysis and Anaïs Bellanger for model drawing. We acknowledge Virginie Georget and Sylvain de Rossi from the Montpellier Imaging Facility MRI, member of the national infrastructure France-BioImaging infrastructure and the Tomsk Regional Common Use Center.

Competing interests

The authors declare no competing or financial interests.

Author contributions

Conceptualization: D.P.; Methodology: D.P., F.C.; Validation: D.P., E.R.M., F.C.; Formal analysis: D.P., F.C.; Investigation: D.P., E.R.M., M.G., F.C.,S.V., L.T., S.B.; Resources: S.L., P.C.; Writing – original draft preparation: C.G-R.; Writing – review and editing: S.L., S.P.; Visualization: D.P., E.R.M., F.C., S.V., E.D., L.T., V.P., S.P., C.G.-R.; Supervision: I.B. (of S.V.), E.D. (of L.T.), V.P (of L.T.), S.P., C.G.-R.; Project administration: C.G.-R.; Funding acquisition: E.D., V.P., C.G.-R.

Funding

This work was supported by the Institut National du Cancer (INCa_9483) and the Russian Science Foundation (14-15-00318). Montpellier Imaging Facility is supported by the Agence Nationale de la Recherche (ANR-10-INBS-04, 'Investments for the future'). The Tomsk Regional Common Use Center is supported by the Russian Science Foundation (14.594.21.0001). C.G.-R. was supported by Institut National de la Santé et de la Recherche Médicale and D.P. by the Fondation pour la Recherche Médicale.

Supplementary information

Supplementary information available online at
http://jcs.biologists.org/lookup/doi/10.1242/jcs.218925.supplemental

References

Aït-Slimane, T., Galmes, R., Trugnan, G. and Maurice, M. (2009). Basolateral internalization of GPI-anchored proteins occurs via a clathrin-independent flotillin-dependent pathway in polarized hepatic cells. *Mol. Biol. Cell* **20**, 3792-3800.

Alonso-Curbelo, D., Riveiro-Falkenbach, E., Pérez-Guijarro, E., Cifdaloz, M., Karras, P., Osterloh, L., Megías, D., Cañón, E., Calvo, T. G., Olmeda, D. et al. (2014). RAB7 controls melanoma progression by exploiting a lineage-specific wiring of the endolysosomal pathway. *Cancer Cell* **26**, 61-76.

Annabi, B., Lachambre, M.-P., Bousquet-Gagnon, N., Pagé, M., Gingras, D. and Béliveau, R. (2001). Localization of membrane-type 1 matrix metalloproteinase in caveolae membrane domains. *Biochem. J.* **353**, 547-553.

Arkhipova, K. A., Sheyderman, A. N., Laktionov, K. K., Mochalnikova, V. V. and Zborovskaya, I. B. (2014). Simultaneous expression of flotillin-1, flotillin-2, stomatin and caveolin-1 in non-small cell lung cancer and soft tissue sarcomas. *BMC Cancer* **14**, 100.

Baldassarre, T., Watt, K., Truesdell, P., Meens, J., Schneider, M. M., Sengupta, S. K. and Craig, A. W. (2015). Endophilin A2 promotes TNBC cell invasion and tumor metastasis. *Mol. Cancer Res.* **13**, 1044-1055.

Berger, T., Ueda, T., Arpaia, E., Chio, I. I. C., Shirdel, E. A., Jurisica, I., Hamada, K., You-Ten, A., Haight, J., Wakeham, A. et al. (2013). Flotillin-2 deficiency leads to reduced lung metastases in a mouse breast cancer model. *Oncogene* **32**, 4989-4994.

Bickel, P. E., Scherer, P. E., Schnitzer, J. E., Oh, P., Lisanti, M. P. and Lodish, H. F. (1997). Flotillin and epidermal surface antigen define a new family of caveolae-associated integral membrane proteins. *J. Biol. Chem.* **272**, 13793-13802.

Bièche, I., Onody, P., Laurendeau, I., Olivi, M., Vidaud, D., Lidereau, R. and Vidaud, M. (1999). Real-time reverse transcription-PCR assay for future management of ERBB2-based clinical applications. *Clin. Chem.* **45**, 1148-1156.

Bloom, H. J. and Richardson, W. W. (1957). Histological grading and prognosis in breast cancer; a study of 1409 cases of which 359 have been followed for 15 years. *Br. J. Cancer* **11**, 359-377.

Bodin, S., Planchon, D., Rios Morris, E., Comunale, F. and Gauthier-Rouviere, C. (2014). Flotillins in intercellular adhesion - from cellular physiology to human diseases. *J. Cell Sci.* **127**, 5139-5147.

Bravo-Cordero, J. J., Marrero-Diaz, R., Megías, D., Genís, L., García-Grande, A., García, M. A., Arroyo, A. G. and Montoya, M. C. (2007). MT1-MMP proinvasive activity is regulated by a novel Rab8-dependent exocytic pathway. *EMBO J.* **26**, 1499-1510.

Cao, S., Cui, Y., Xiao, H., Mai, M., Wang, C., Xie, S., Yang, J., Wu, S., Li, J., Song, L. et al. (2016). Upregulation of flotillin-1 promotes invasion and metastasis by activating TGF-β signaling in nasopharyngeal carcinoma. *Oncotarget* **7**, 4252-4264.

Castro-Castro, A., Marchesin, V., Monteiro, P., Lodillinsky, C., Rossé, C. and Chavrier, P. (2016). Cellular and molecular mechanisms of MT1-MMP-dependent cancer cell invasion. *Annu. Rev. Cell Dev. Biol.* **32**, 555-576.

Causeret, M., Taulet, N., Comunale, F., Favard, C. and Gauthier-Rouvière, C. (2005). N-cadherin association with lipid rafts regulates its dynamic assembly at cell-cell junctions in C2C12 myoblasts. *Mol. Biol. Cell* **16**, 2168-2180.

Charrasse, S., Comunale, F., Grumbach, Y., Poulat, F., Blangy, A. and Gauthier-Rouvière, C. (2006). RhoA GTPase regulates M-cadherin activity and myoblast fusion. *Mol. Biol. Cell* **17**, 749-759.

Chevalier, C., Collin, G., Descamps, S., Touaitahuata, H., Simon, V., Reymond, N., Fernandez, L., Milhiet, P.-E., Georget, V., Urbach, S. et al. (2016). TOM1L1 drives membrane delivery of MT1-MMP to promote ERBB2-induced breast cancer cell invasion. *Nat. Commun.* **7**, 10765.

Coates, A. S., Winer, E. P., Goldhirsch, A., Gelber, R. D., Gnant, M., Piccart-Gebhart, M., Thurlimann, B. and Senn, H.-J. (2015). Tailoring therapies–improving the management of early breast cancer: St Gallen international expert consensus on the primary therapy of early breast cancer 2015. *Ann. Oncol.* **26**, 1533-1546.

Cornfine, S., Himmel, M., Kopp, P., El Azzouzi, K., Wiesner, C., Krüger, M., Rudel, T. and Linder, S. (2011). The kinesin KIF9 and reggie/flotillin proteins regulate matrix degradation by macrophage podosomes. *Mol. Biol. Cell* **22**, 202-215.

Costes, S. V., Daelemans, D., Cho, E. H., Dobbin, Z., Pavlakis, G. and Lockett, S. (2004). Automatic and quantitative measurement of protein-protein colocalization in live cells. *Biophys. J.* **86**, 3993-4003.

Dozynkiewicz, M. A., Jamieson, N. B., MacPherson, I., Grindlay, J., van den Berghe, P. V. E., von Thun, A., Morton, J. P., Gourley, C., Timpson, P., Nixon, C. et al. (2012). Rab25 and CLIC3 collaborate to promote integrin recycling from late endosomes/lysosomes and drive cancer progression. *Dev. Cell* **22**, 131-145.

Fortier, M., Comunale, F., Kucharczak, J., Blangy, A., Charrasse, S. and Gauthier-Rouviere, C. (2008). RhoE controls myoblast alignment prior fusion through RhoA and ROCK. *Cell Death Differ.* **15**, 1221-1231.

Frick, M., Bright, N. A., Riento, K., Bray, A., Merrified, C. and Nichols, B. J. (2007). Coassembly of flotillins induces formation of membrane microdomains, membrane curvature, and vesicle budding. *Curr. Biol.* **17**, 1151-1156.

Friedl, P. and Wolf, K. (2010). Plasticity of cell migration: a multiscale tuning model. *J. Cell Biol.* **188**, 11-19.

Frittoli, E., Palamidessi, A., Disanza, A. and Scita, G. (2011). Secretory and endo/exocytic trafficking in invadopodia formation: the MT1-MMP paradigm. *Eur. J. Cell Biol.* **90**, 108-114.

Frittoli, E., Palamidessi, A., Marighetti, P., Confalonieri, S., Bianchi, F., Malinverno, C., Mazzarol, G., Viale, G., Martin-Padura, I., Garré, M. et al. (2014). A RAB5/RAB4 recycling circuitry induces a proteolytic invasive program and promotes tumor dissemination. *J. Cell Biol.* **206**, 307-328.

Galvez, B. G., Matías-Román, S., Yáñez-Mó, M., Vicente-Manzanares, M., Sánchez-Madrid, F. and Arroyo, A. G. (2003). Caveolae are a novel pathway for membrane-type 1 matrix metalloproteinase traffic in human endothelial cells. *Mol. Biol. Cell* **15**, 678-687.

Ge, L., Qi, W., Wang, L.-J., Miao, H.-H., Qu, Y.-X., Li, B.-L. and Song, B.-L. (2011). Flotillins play an essential role in Niemann-Pick C1-like 1-mediated cholesterol uptake. *Proc. Natl. Acad. Sci. USA* **108**, 551-556.

Glebov, O. O., Bright, N. A. and Nichols, B. J. (2006). Flotillin-1 defines a clathrin-independent endocytic pathway in mammalian cells. *Nat. Cell Biol.* **8**, 46-54.

Guillaume, E., Comunale, F., Do Khoa, N., Planchon, D., Bodin, S. and Gauthier-Rouviere, C. (2013). Flotillin microdomains stabilize cadherins at cell-cell junctions. *J. Cell Sci.* **126**, 5293-5304.

Hazarika, P., McCarty, M. F., Prieto, V. G., George, S., Babu, D., Koul, D., Bar-Eli, M. and Duvic, M. (2004). Up-regulation of flotillin-2 is associated with melanoma progression and modulates expression of the thrombin receptor protease activated receptor 1. *Cancer Res.* **64**, 7361-7369.

Hofmann, U. B., Eggert, A. A. O., Blass, K., Bröcker, E.-B. and Becker, J. C. (2003). Expression of matrix metalloproteinases in the microenvironment of spontaneous and experimental melanoma metastases reflects the requirements for tumor formation. *Cancer Res.* **63**, 8221-8225.

Hoshino, D., Kirkbride, K. C., Costello, K., Clark, E. S., Sinha, S., Grega-Larson, N., Tyska, M. J. and Weaver, A. M. (2013). Exosome secretion is enhanced by invadopodia and drives invasive behavior. *Cell Rep.* **5**, 1159-1168.

Hotary, K., Li, X.-Y., Allen, E., Stevens, S. L. and Weiss, S. J. (2006). A cancer cell metalloprotease triad regulates the basement membrane transmigration program. *Genes Dev.* **20**, 2673-2686.

Kajiho, H., Kajiho, Y., Frittoli, E., Confalonieri, S., Bertalot, G., Viale, G., Di Fiore, P. P., Oldani, A., Garre, M., Beznoussenko, G. V. et al. (2016). RAB2A controls MT1-MMP endocytic and E-cadherin polarized Golgi trafficking to promote invasive breast cancer programs. *EMBO Rep.* **17**, 1061-1080.

Kinsel, L. B., Szabo, E., Greene, G. L., Konrath, J., Leight, G. S. and McCarty, K. S. Jr. (1989). Immunocytochemical analysis of estrogen receptors as a predictor of prognosis in breast cancer patients: comparison with quantitative biochemical methods. *Cancer Res.* **49**, 1052-1056.

Koh, M., Yong, H.-Y., Kim, E.-S., Son, H., Jeon, Y. R., Hwang, J.-S., Kim, M.-O., Cha, Y., Choi, W. S., Noh, D.-Y. et al. (2016). A novel role for flotillin-1 in H-Ras-regulated breast cancer aggressiveness: flotillin-1 is important for breast cancer aggressiveness. *Int. J. Cancer* **138**, 1232-1245.

Lakhani, S. R., Ellis, I. O., Schnitt, S. J., Tan, P. H. and van de Vijver, M. J. (2012). *World Health Organization (WHO) Classification of Tumours of the Breast*. IARC Press, Lyon, France.

Lang, D. M., Lommel, S., Jung, M., Ankerhold, R., Petrausch, B., Laessing, U., Wiechers, M. F., Plattner, H. and Stuermer, C. A. (1998). Identification of reggie-1 and reggie-2 as plasmamembrane-associated proteins which cocluster with activated GPI-anchored cell adhesion molecules in non-caveolar micropatches in neurons. *J. Neurobiol.* **37**, 502-523.

Leong, H. S., Robertson, A. E., Stoletov, K., Leith, S. J., Chin, C. A., Chien, A. E., Hague, M. N., Ablack, A., Carmine-Simmen, K., McPherson, V. A. et al. (2014). Invadopodia are required for cancer cell extravasation and are a therapeutic target for metastasis. *Cell Rep.* **8**, 1558-1570.

Li, H., Wang, R.-M., Liu, S.-G., Zhang, J.-P., Luo, J.-Y., Zhang, B.-J. and Zhang, X.-G. (2014). Abnormal expression of FLOT1 correlates with tumor progression and poor survival in patients with non-small cell lung cancer. *Tumor Biol.* **35**, 3311-3315.

Lin, C., Wu, Z., Lin, X., Yu, C., Shi, T., Zeng, Y., Wang, X., Li, J. and Song, L. (2011). Knockdown of FLOT1 impairs cell proliferation and tumorigenicity in breast cancer through upregulation of FOXO3a. *Clin. Cancer Res.* **17**, 3089-3099.

Linder, S., Wiesner, C. and Himmel, M. (2011). Degrading devices: invadosomes in proteolytic cell invasion. *Annu. Rev. Cell Dev. Biol.* **27**, 185-211.

Liu, J., Huang, W., Ren, C., Wen, Q., Liu, W., Yang, X., Wang, L., Zhu, B., Zeng, L., Feng, X. et al. (2015a). Flotillin-2 promotes metastasis of nasopharyngeal carcinoma by activating NF-kappaB and PI3K/Akt3 signaling pathways. *Sci. Rep.* **5**, 11614.

Liu, Y., Lin, L., Huang, Z., Ji, B., Mei, S., Lin, Y. and Shen, Z. (2015b). High expression of flotillin-2 is associated with poor clinical survival in cervical carcinoma. *Int. J. Clin. Exp. Pathol.* **8**, 622-628.

Lodillinsky, C., Infante, E., Guichard, A., Chaligné, R., Fuhrmann, L., Cyrta, J., Irondelle, M., Lagoutte, E., Vacher, S., Bonsang-Kitzis, H. et al. (2016). p63/MT1-MMP axis is required for in situ to invasive transition in basal-like breast cancer. *Oncogene* **35**, 344-357.

Macpherson, I. R., Rainero, E., Mitchell, L. E., van den Berghe, P. V. E., Speirs, C., Dozynkiewicz, M. A., Chaudhary, S., Kalna, G., Edwards, J., Timpson, P. et al. (2014). CLIC3 controls recycling of late endosomal MT1-MMP and dictates invasion and metastasis in breast cancer. *J. Cell Sci.* **127**, 3893-3901.

Monteiro, P., Rossé, C., Castro-Castro, A., Irondelle, M., Lagoutte, E., Paul-Gilloteaux, P., Desnos, C., Formstecher, E., Darchen, F., Perrais, D. et al. (2013). Endosomal WASH and exocyst complexes control exocytosis of MT1-MMP at invadopodia. *J. Cell Biol.* **203**, 1063-1079.

Otto, G. P. and Nichols, B. J. (2011). The roles of flotillin microdomains-endocytosis and beyond. *J. Cell Sci.* **124**, 3933-3940.

Parton, R. G. and del Pozo, M. A. (2013). Caveolae as plasma membrane sensors, protectors and organizers. *Nat. Rev. Mol. Cell Biol.* **14**, 98-112.

Poincloux, R., Lizarraga, F. and Chavrier, P. (2009). Matrix invasion by tumour cells: a focus on MT1-MMP trafficking to invadopodia. *J. Cell Sci.* **122**, 3015-3024.

Pust, S., Klokk, T. I., Musa, N., Jenstad, M., Risberg, B., Erikstein, B., Tcatchoff, L., Liestøl, K., Danielsen, H. E., van Deurs, B. et al. (2013). Flotillins as regulators of ErbB2 levels in breast cancer. *Oncogene* **32**, 3443-3451.

Rainero, E. and Norman, J. C. (2013). Late endosomal and lysosomal trafficking during integrin-mediated cell migration and invasion: cell matrix receptors are trafficked through the late endosomal pathway in a way that dictates how cells migrate. *BioEssays* **35**, 523-532.

Ran, F. A., Hsu, P. D., Wright, J., Agarwala, V., Scott, D. A. and Zhang, F. (2013). Genome engineering using the CRISPR-Cas9 system. *Nat. Protoc.* **8**, 2281-2308.

Remacle, A., Murphy, G. and Roghi, C. (2003). Membrane type I-matrix metalloproteinase (MT1-MMP) is internalised by two different pathways and is recycled to the cell surface. *J. Cell Sci.* **116**, 3905-3916.

Rivera-Milla, E., Stuermer, C. A. O. and Malaga-Trillo, E. (2006). Ancient origin of reggie (flotillin), reggie-like, and other lipid-raft proteins: convergent evolution of the SPFH domain. *Cell. Mol. Life Sci.* **63**, 343-357.

Rosse, C., Lodillinsky, C., Fuhrmann, L., Nourieh, M., Monteiro, P., Irondelle, M., Lagoutte, E., Vacher, S., Waharte, F., Paul-Gilloteaux, P. et al. (2014). Control of MT1-MMP transport by atypical PKC during breast-cancer progression. *Proc. Natl. Acad. Sci. USA* **111**, E1872-E1879.

Rowe, R. G. and Weiss, S. J. (2009). Navigating ECM barriers at the invasive front: the cancer cell-stroma interface. *Annu. Rev. Cell Dev. Biol.* **25**, 567-595.

Sabeh, F., Ota, I., Holmbeck, K., Birkedal-Hansen, H., Soloway, P., Balbin, M., Lopez-Otin, C., Shapiro, S., Inada, M., Krane, S. et al. (2004). Tumor cell traffic through the extracellular matrix is controlled by the membrane-anchored collagenase MT1-MMP. *J. Cell Biol.* **167**, 769-781.

Schneider, A., Rajendran, L., Honsho, M., Gralle, M., Donnert, G., Wouters, F., Hell, S. W. and Simons, M. (2008). Flotillin-dependent clustering of the amyloid precursor protein regulates its endocytosis and amyloidogenic processing in neurons. *J. Neurosci.* **28**, 2874-2882.

Sigismund, S., Confalonieri, S., Ciliberto, A., Polo, S., Scita, G. and Di Fiore, P. P. (2012). Endocytosis and signaling: cell logistics shape the eukaryotic cell plan. *Physiol. Rev.* **92**, 273-366.

Steffen, A., Le Dez, G., Poincloux, R., Recchi, C., Nassoy, P., Rottner, K., Galli, T. and Chavrier, P. (2008). MT1-MMP-dependent invasion is regulated by TI-VAMP/VAMP7. *Curr. Biol.* **18**, 926-931.

Sung, B. H., Ketova, T., Hoshino, D., Zijlstra, A. and Weaver, A. M. (2015). Directional cell movement through tissues is controlled by exosome secretion. *Nat. Commun.* **6**, 7164.

Thuault, S., Hayashi, S., Lagirand-Cantaloube, J., Plutoni, C., Comunale, F., Delattre, O., Relaix, F. and Gauthier-Rouvière, C. (2013). P-cadherin is a direct PAX3-FOXO1A target involved in alveolar rhabdomyosarcoma aggressiveness. *Oncogene* **32**, 1876-1887.

Uekita, T., Itoh, Y., Yana, I., Ohno, H. and Seiki, M. (2001). Cytoplasmic tail–dependent internalization of membrane-type 1 matrix metalloproteinase is important for its invasion-promoting activity. *J. Cell Biol.* **155**, 1345-1356.

Ueno, H., Nakamura, H., Inoue, M., Imai, K., Noguchi, M., Sato, H., Seiki, M. and Okada, Y. (1997). Expression and tissue localization of membrane-types 1, 2, and 3 matrix metalloproteinases in human invasive breast carcinomas. *Cancer Res.* **57**, 2055-2060.

Wang, X., Yang, Q., Guo, L., Li, X.-H., Zhao, X.-H., Song, L.-B. and Lin, H.-X. (2013). Flotillin-2 is associated with breast cancer progression and poor survival outcomes. *J. Transl. Med.* **11**, 190.

Williams, K. C. and Coppolino, M. G. (2011). Phosphorylation of membrane type 1-matrix metalloproteinase (MT1-MMP) and its vesicle-associated membrane protein 7 (VAMP7)-dependent trafficking facilitate cell invasion and migration. *J. Biol. Chem.* **286**, 43405-43416.

Williamson, D., Missiaglia, E., de Reyniès, A., Pierron, G., Thuille, B., Palenzuela, G., Thway, K., Orbach, D., Laé, M., Fréneaux, P. et al. (2010). Fusion gene-negative alveolar rhabdomyosarcoma is clinically and molecularly indistinguishable from embryonal rhabdomyosarcoma. *J. Clin. Oncol.* **28**, 2151-2158.

Wolf, K., Wu, Y. I., Liu, Y., Geiger, J., Tam, E., Overall, C., Stack, M. S. and Friedl, P. (2007). Multi-step pericellular proteolysis controls the transition from individual to collective cancer cell invasion. *Nat. Cell Biol.* **9**, 893-904.

Wolf, K., Te Lindert, M., Krause, M., Alexander, S., Te Riet, J., Willis, A. L., Hoffman, R. M., Figdor, C. G., Weiss, S. J. and Friedl, P. (2013). Physical limits of cell migration: control by ECM space and nuclear deformation and tuning by proteolysis and traction force. *J. Cell Biol.* **201**, 1069-1084.

Wolff, A. C., Hammond, M. E., Schwartz, J. N., Hagerty, K. L., Allred, D. C., Cote, R. J., Dowsett, M., Fitzgibbons, P. L., Hanna, W. M., Langer, A. et al. (2007). American society of clinical oncology/college of american pathologists guideline recommendations for human epidermal growth factor receptor 2 testing in breast cancer. *Arch. Pathol. Lab. Med.* **131**, 18-43.

Yamaguchi, H., Takeo, Y., Yoshida, S., Kouchi, Z., Nakamura, Y. and Fukami, K. (2009). Lipid rafts and caveolin-1 are required for invadopodia formation and extracellular matrix degradation by human breast cancer cells. *Cancer Res.* **69**, 8594-8602.

Yan, Y., Yang, F.-Q., Zhang, H.-M., Che, J. and Zheng, J.-H. (2014). Up-regulation of flotillin-2 is associated with renal cell carcinoma progression. *Tumor Biol.* **35**, 10479-10486.

Yu, X., Zech, T., McDonald, L., Gonzalez, E. G., Li, A., Macpherson, I., Schwarz, J. P., Spence, H., Futo, K., Timpson, P. et al. (2012). N-WASP coordinates the delivery and F-actin-mediated capture of MT1-MMP at invasive pseudopods. *J. Cell Biol.* **199**, 527-544.

Zavyalova, M. V., Denisov, E. V., Tashireva, L. A., Gerashchenko, T. S., Litviakov, N. V., Skryabin, N. A., Vtorushin, S. V., Telegina, N. S., Slonimskaya, E. M., Cherdyntseva, N. V. and Perelmuter, V. M. (2013). Phenotypic drift as a cause for intratumoral morphological heterogeneity of invasive ductal breast carcinoma not otherwise specified. *BioRes. Open Access* **2**, 148-154.

Zhang, S.-H., Wang, C.-J., Shi, L., Li, X.-H., Zhou, J., Song, L.-B. and Liao, W.-T. (2013). High expression of FLOT1 is associated with progression and poor prognosis in hepatocellular carcinoma. *PLoS ONE* **8**, e64709.

Zhang, Y., Li, J., Song, Y., Chen, F., Pei, Y. and Yao, F. (2014). Flotillin-1 expression in human clear-cell renal cell carcinoma is associated with cancer progression and poor patient survival. *Mol. Med. Rep.* **10**, 860-866.

Zhao, L., Lin, L., Pan, C., Shi, M., Liao, Y., Bin, J. and Liao, W. (2015). Flotillin-2 promotes nasopharyngeal carcinoma metastasis and is necessary for the epithelial-mesenchymal transition induced by transforming growth factor-β. *Oncotarget* **6**, 9781-9793.

Zhu, Z., Wang, J., Sun, Z., Sun, X., Wang, Z. and Xu, H. (2013). Flotillin2 expression correlates with HER2 levels and poor prognosis in gastric cancer. *PLoS ONE* **8**, e62365.